Exploring the role of nanocellulose as potential sustainable material for enhanced oil recovery

Rana, Ashvinder K.; Thakur, Manju Kumari; Gupta, Vijai Kumar; Thakur, Vijay Kumar

Exploring the role of nanocellulose as potential sustainable material for enhanced oil recovery: New paradigm for a circular economy

Ashvinder K. Rana [a,b,*], Manju Kumari Thakur [c], Vijai Kumar Gupta [a], Vijay Kumar Thakur [a,**,1]

[a] Biorefining and Advanced Materials Research Center, SRUC, Kings Buildings, West Mains Road, Edinburgh, UK
[b] Department of Chemistry, Sri Sai University, Palampur 176061, India
[c] Department of Chemistry, RNT Govt College Sarkaghat, Distt Mandi, HP, India

ARTICLE INFO

ABSTRACT

Presently, due to growing global energy demand and depletion of existing oil reservoirs, oil industry is focussing on development of novel and effective ways to enhance crude oil recovery and exploration of new oil reserves, which are typically found in challenging environment and require deep drilling in high temperature and high-pressure regime. The nanocelluloses with numerous advantages such as high temperature and pressure stability, ecofriendly nature, excellent rheology modifying ability, interfacial tension reduction capability, etc., have shown a huge potential in oil recovery over conventional chemicals and macro/micro sized biopolymers-based approach.

In present review, an attempt has been made to thoroughly investigate the potential of nanocellulose (cellulose nanocrystals/nanofibers) in development of drilling fluid and in enhancement of oil recovery. The impact of various factors such as nanocellulose shape, charge density, inter-particle or inter-fibers interactions after surface functionalization, rheometer geometries, additives, post processing techniques, etc., which provides insight into the attributes of nanocellulose suspension and exemplify their behaviour during oil recovery have also been reviewed and discussed. Finally, the conclusion and challenges in utility of nanocellulose for oilfield applications are addressed. Knowing how to adjust/quantify nanocrystals/nanofibers shape and size; and monitor their interactions might promote their utility in oilfield industry.

1. Introduction

Traditionally, many chemical reagents have been used in the development of the oilfield industry, such as in oil recovery and fluid drilling (Bist et al., 2023; Wang et al., 2021). However, due to their toxicity, low environmental adaptation, non-biodegradability, and instability at elevated temperatures, scientists are currently looking for greener, highly efficient, inexpensive, and non-toxic biomaterials for the sustained development of oilfields (He et al., 2016; M.-C. Li et al., 2023a, 2023b; ÜNAL KIZILIRMAK, 2023; Wang et al., 2021). The highly abundantly available biopolymer cellulose, in its macro as well as nano form, has been utilized for a long time in numerous fields, such as in the medical, food, composite, and energy sectors (Rana, 2023; Rana et al., 2022c; Rana and Thakur, 2023; Trache et al., 2020) (Ates et al., 2020; Singha and Thakur, 2009; Thakur et al., 2013). However, its use in the

oil industry has proliferated in the last seven to eight years. Since nanocellulose (NCs) satisfies technical and all other aforementioned requirements, and thus has been preferred over traditional chemical reagents by scientists in the oilfield industry. In addition, the availability of a wide range of sources, recyclable, hydrophilic nature, controlled functionalization, and less damage to the formation are some of the other reasons contributing to their growing popularity in the oil industry (Rana, 2022; Rana et al., 2024, 2022a).

NCs extracted from biomasses, including cellulose nano crystals (CNCs) and cellulose nano fibres (CNFs), possess several unique properties and can be manufactured on a vast scale with a wide variety of functional groups (Beluns et al., 2021; Neibolts et al., 2020; Platnieks et al., 2021; Zielińska et al., 2021). With the revolutionary works of Revol et al. (Revol et al., 1992) on nematic self-ordering of CNCs in aqueous suspension and Herrick et al. (Herrick et al., 1983) on

---

describing the shear thinning behaviour of 2% (w/w) CNFs suspension in water, both CNCs and CNFs have received considerable interest from researchers as well as engineers working in different fields.

NCs, as advanced materials, possess high tensile strength, are biocompatible and biodegradable, abundant, non-toxic, have good thermal strength, and are economical (Dong et al., 2023; Eichhorn, 2011; James et al., 2023). Furthermore, NC suspensions exhibit distinctive and attractive rheological features due to their higher aspect ratio and the presence of an abundance of OH groups on their surface. In CNCs, isotropic suspension is observed at low concentrations, followed by chiral nematic liquid crystalline structure within a specific concentration range, and gelation at higher concentrations. Moreover, CNCs are more effective in creating yield stress, gel strength in suspension, and low-shear viscosity (Li et al., 2021). Contrarily, CNFs show higher viscosities when their concentrations are increased, or their fibrillation rates are elevated (Biliuta et al., 2023a; Kim et al., 2023; Saarikoski et al., 2012). The fibrillation raises the surface area of CNFs, which in turn enhances the contacts between nanofibers, causing the fibril to agglomerate or form flocs and thus increase the viscosity of suspension. In addition to having some characteristics of soft glassy materials (such as colloidal gels, concentrated emulsions, and clay suspensions), CNFs also exhibit characteristics typical to that of non-colloidal and colloidal suspensions, in which the imposed strain can destabilise and reconfigure the material's structure (Biliuta et al., 2023a; Carneiro Pessan et al., 2023; Derakhshandeh et al., 2011; Martoïa et al., 2015). The CNF flocs, alignment, movement from solid boundaries, and considerable time dependence of such systems make rheological observations challenging (Dimic-Misic et al., 2014).

NC, due to its interesting viscoelastic properties, has the potential to be exploited for rheological control in a wide range of application areas, including food and cosmetics products(Armstrong et al., 2022; Lee et al., 2022), drilling fluids (S. Wang et al., 2022a,2022b), polymer industry (Ren et al., 2022), bio-medical field (Olmos-Juste et al., 2021), bone and tissue engineering (Kam et al., 2021), etc. (Fig. 1).

In petroleum/oil industry, NC has been used as a plugging agent, fluid loss and rheology modifier agent in drilling fluid; and as stable emulsion agent, foaming agent, nano-oil displacing agent in enhanced oil recovery method (Hou et al., 2022; ÜNAL KIZILIRMAK, 2023; Zhu

et al., 2021). A couple of review articles have been published highlighting the role and capability of NCs in oil and gas production (Combariza et al., 2021; Isaac et al., 2022; Wang et al., 2021). But, in present review article we will mainly focus on recent advancement in utility of NCs as an additive in drilling fluid and its role as foam stabilising agents, emulsion stabilising, oil displacing in enhanced oil recovery technique for better oil productivity. Further, it is also vital to comprehend how interparticle/fibril forces affect the underlying nanostructure of these materials to optimise their capability of modulating the rheology of fluids in oil sector as well as in other areas. Thus, this review article will also provide an insight for the beginners a detailed view on how structure and rheology of NC suspensions in aqueous media can be mapped as a function of time, temperature, zeta potential, electrolyte, inorganic particle addition, pH, salt, crowding factor, etc. Because of its exceptional mechanical and rheological properties, NC is viable alternative to standard chemical-based and synthetic polymers based approaches for improved oil recovery (Wang et al., 2021) and thus may facilitate a transition to circular bioeconomy concept, while also providing sustainable solutions for waste management.

2. Introduction to some basic terms in rheology

Shear and stress are the two terms that make up shear stress. Shear refers to the relative movement of adjacent parallel layers. A movement across parallel layers happens when an object is dragged over a surface (Fig. 2a). The term stress, conversely, is defined as the force applied to a surface divided by the area across which the force was exerted. Shear stress (τ) is one type of stress. It occurs when parallel layers of a matter move successively in the plane of shear under the applied stress. Rheological measurements involve forcing a sample to move through an instrument utilising a measuring geometry (Goodwin and Hughes, 2008; Wahlkrantz, 2020). The τ can be calculated using the equation given below (Mezger, 2006).

$$\tau = F/A$$

Here, τ = shear stress (Pa); F = applied force (N); and A = area (m^2).

Shear strain (γ) illustrates the relative in-plane movement of two parallel layers. It is the ratio of the deformation of a fluid in one direction to the length of the perpendicular axis. The length of the perpendicular axis is simply the distance between the plates when the material is positioned between two parallel plates, and only one of the plates moves (Fig. 2b). It is computed using the following equation (Mezger, 2006).

$$\gamma = v/h \ (s^{-1})$$

Here, v and h are the velocity of u (m/s) and distance between plates (metres), respectively.

Measuring geometry's speed in a rheometer is regulated to get the required shear rate. The ratio of shear strain to time gives the shear rate ($\dot{\gamma}$), which is also called the rate of shear strain. Shear viscosity, η (Pa s), is one of the most commonly described rheological properties and is defined as the ratio of τ and $\dot{\gamma}$. In fluids, all molecules move relative to each other, and their relative motion due to frictional internal forces creates a resistance to their flow. This flow resistance is defined as the shear viscosity of the fluid (Mezger, 2006).

When a fluid shows an ideally viscous flow behavior, i.e., a linear relationship between shear stress and shear strain, it is called a Newtonian liquid. Unlike Newtonian fluids, non-Newtonian fluids exhibit a nonlinear relation between the shear stress and shear rate (Fig. 2c). These fluids possess shear-rate-dependent rheological characteristics, i. e., shear-thinning or shear-thickening properties, and their viscosity varies with shear stress. Shear thinning means a decrease in viscosity, whereas shear thickening means that the viscosity of fluids increases with an increase in shear stress or strain. Tang et al. (Tang et al., 2018) reported three region shear thinning behaviour for cationically (glycidyltrimethylammonium chloride) modified CNCs, which include
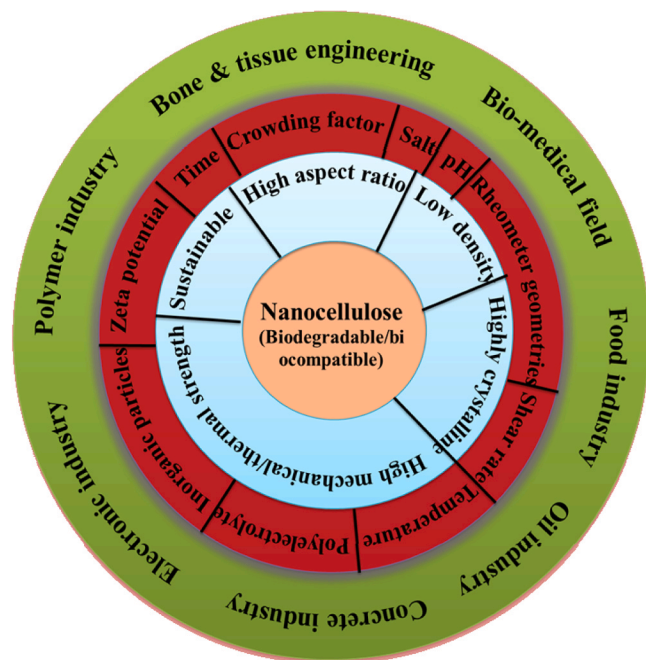

Fig. 1. Properties, factors impacting the rheology and applications of NC in various fields.
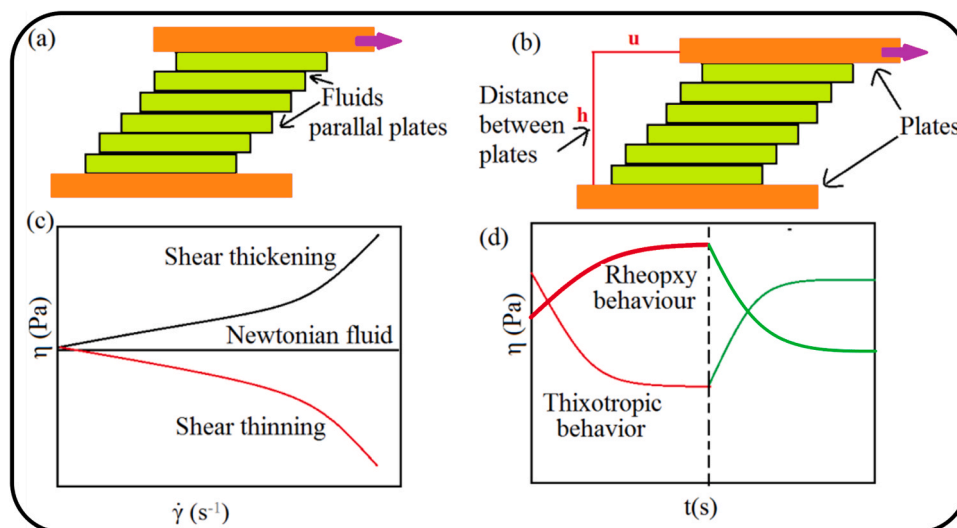
Fig. 2. Illustrates (a) shear stress, (b) the distance (h) between plates and deformation (u) utilized to calculate shear strain, (c) the behavior of Newtonian and Non-Newtonian fluids, (d) thixotropic behavior and rheopxy behaviour (Mezger, 2006). (in figure d, red and green lines represent the viscosity curve when shear stress is applied, and the green line represents the behaviour of fluids after removal of shear load). Adapted with permission from Ref. (Mezger, 2006).

shear-thinning at a low shear rate, shear thickening at intermediate and shear thinning at higher shear rates.

Most of the fluids are thixotropic by nature, which means they exhibit a reversible decrement in their viscosity at a particular shear stress. Biliuta et al. (Biliuta et al., 2023a) extracted 2,2,6,6-tetramethyl-piperidine-1-oxyl radical (TEMPO) oxidized CNFs (TO-CNFs) from different kinds of commercially available cellulose namely, alpha cellulose, microcrystalline cellulose (MCC), eucalyptus and cotton linters via TEMPO mediated oxidation of preactivated samples (activated using combined alkaline-acid treatment) and subsequently compared their rheological properties. TO-CNFs extracted from alpha cellulose showed highest viscosity, yield stress and thxiotropy followed by MCC-CNFs, eucalyptus-based CNFs and cotton linters-CNFs. In addition, the optimized sample i.e., alpha- CNFs also exhibited strong ability to recover after a high level of deformation. Contrary to thixotropy, in rheopexy, the fluid viscosity increases with an increase in shear load and upon rest system breakdown. Rheopexy and thixotropy are time-dependent rheological behaviours, and to determine them, both deterioration and the regeneration of the network need to be taken into consideration. Typical viscosity curves showing thixotropic/rheopexy behaviour are given in Fig. 2d.

When the applied shear stress exceeds the fluid internal forces, the yield point occurs, i.e., the system deforms from an elastic to a viscoelastic form (showing both viscous and elastic behaviour) (Hackley and Ferraris, 2001). The elastic and viscous parts of viscoelastic materials are represented by storage modulus (G') and loss modulus (G''), respectively. Under constant stress, viscoelastic materials exhibit a viscous flow and lose some of their energy. However, when stress is released, a part of the stored mechanical energy results in the recovery of materials to their initial state because of the elastic behavior. Material can be categorized as a viscoelastic liquid (having loss modulus> storage modulus), a viscoelastic solid (having storage modulus >loss modulus) or a gel (loss modulus= storage modulus).

3. Cellulose, nanocellulose and production of nanocellulose

Cellulose is one of the most prevalent biopolymers on the planet. It is easily accessible, biodegradable, environmentally friendly, semi-crystalline and naturally hydrophilic. Cellulose is found primarily in plants, trees, algae, and tunicates. However, it can also be synthesised by bacteria (Gatenholm and Klemm, 2010; Moon et al., 2011). It is made up of D-glucose units linked through β − 1,4-glycosidic linkage. Because of

the presence of hydroxyl groups on its surface, the linear cellulose chain possesses a higher degree of stability by forming hydrogen bonding between adjacent chains (Moon et al., 2011; Rana et al., 2021). Van der Waals forces and hydrogen bonding play a significant role in the parallel stacking of cellulose chains, forming elementary fibrils, which, upon further agglomeration, form microfibrils. There are various methods available in literature through which macro/micro cellulose can be easily converted into different nanocellulose (NCs) forms, i.e., cellulose nanocrystals (CNCs) and cellulose nano fibers (CNFs) (Fig. 3)(Michelin et al., 2020; Qing et al., 2013; Xu et al., 2013).

The nanocellulose means cellulose having at least one dimension in the nano range. In addition to CNF and CNCs, as discussed above, there is another NC class named bacterial NC (BC), which, contrary to formers, is synthesised by bacteria (Rana et al., 2021c; Rana et al., 2022b; Rana and Thakur, 2021). Our prime interest in the present article is only on nanocellulose accessible from waste biomasses. The inherent characteristics such as tensile strength, surface geometry, dimensions and crystalline nature of NCs vary with source materials, NCs types and extraction techniques utilized (Rana et al., 2021b; Rana et al., 2021). Both CNCs and CNFs, because of their higher mechanical toughness, nano dimensions, higher thermal stability, low density, tunable surface characteristics, biodegradable nature, high crystallinity and ease of availability, have been tremendously utilised as rheology modifiers agents in numerous fluids for advanced applications. CNCs are comparatively denser (1.6 g/cm^3), highly crystalline (54–88%), much finer (Length: 100–500 nm; Diamet: 2–20 nm), mechanically tougher (Tensile strength:7500–7700 MPa) and have a superior aspect ratio than CNFs (Density:1.5 g/cm^3; crystallinity: 45–80%; Leng: 500–2000 nm & Diamet: 1–100 nm; and tensile strength: 357.5 MPa) (Rana et al., 2021a; Rana et al., 2022a). CNCs are generally synthesized by using organosolv treatment, enzymatic hydrolysis, inorganic acids/organic acids, deep eutectic solvents, ionic liquids, TEMPO-oxidation, mechanical methods, etc (Rana et al., 2021). The most commonly used acids are HCl, H$_2$SO$_4$, HCOOH and phosphoric acid, and the resulting CNCs in the present paper were abbreviated as Hcl-CNCs, Sul-CNCs, Form-CNCs and Pho-CNCs, respectively. The acid hydrolysis techniques remove the amorphous regions, resulting in highly crystalline CNCs with some surface active functional groups. The utility of H$_3$PO4, H$_2$SO$_4$, and oxalic acid (C$_2$H$_2$O$_4$) /TEMPO led towards the grafting of –ve charged functional groups phosphates, sulphate half-esters and carboxylate groups, respectively onto CNCs's surface, which in turn, due to electrostatic repulsion, plays a crucial role defining the rheology of CNCs in aqueous
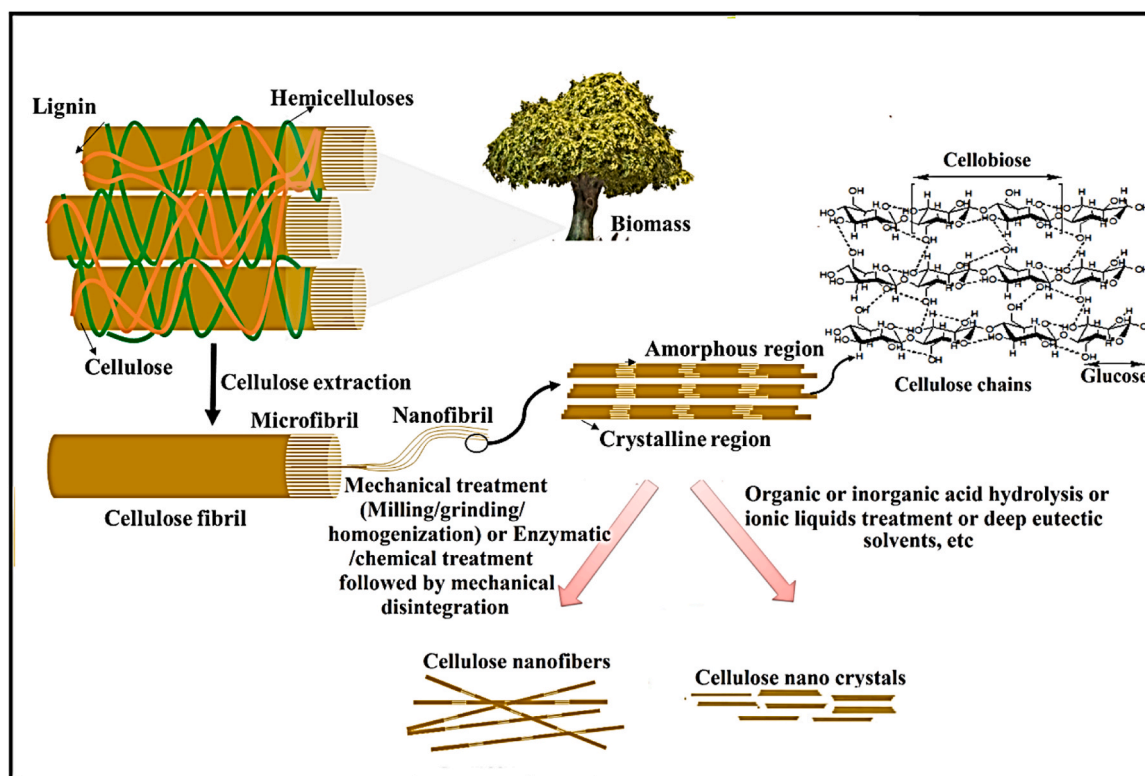
Fig. 3. Process of CNFs and CNCs synthesis. Adapted with permission from Ref. (Michelin et al., 2020).

suspension.

The impact of time, temperature, acid concentration, and the relative ratio of acids and cellulose on active groups density, percent crystallinity and % yield of CNCs have been evaluated by different scientists (Hafemann et al., 2020; Nang An et al., 2020; Sang et al., 2017; Vanderfleet et al., 2018; Wijaya et al., 2020). The amount of sulphate groups on Sul-CNCs was found to vary with H_2SO_4 concentration (increases with increase in acid concentration) as well as the reaction temperature (gives maximum charge density at low temperature). However, no sharp impact of time on sulphate group density was noted. Whereas in the case of Pho-CNCs, and TEMPO-CNCs (TO-CNCs), the density of phosphate groups and carboxyl groups, respectively, depended on time and temperature (Sang et al., 2017; Vanderfleet et al., 2018). CNFs are comparatively longer and, at comparatively low concentrations ($< 1\%$), form viscous suspensions due to highly intertwined structure. CNFs have been extracted from biomasses using mechanical techniques like grinding, milling and homogenization; chemical treatments such as carboxymethylation, TEMPO oxidation, sulfonation, etc.; and chemical/enzymatic pretreatments succeeded by mechanical deterioration (Habibi et al., 2006; Li et al., 2021; Nechyporchuk et al., 2016a; Saito et al., 2007). Here, CNFs synthesized by employing the following pretreatment, namely enzymatic, sulfonation, periodate-chlorite oxidation, carboxymethylation and TEMPO oxidation, before mechanical deterioration of cellulose have been represented as Enz-CNFs, Sul-CNFs, PC-CNFs, CM-CNFs and TO-CNF, respectively.

4. The potential of nanocellulose in the oilfield industry

Owing to NC's intricate surface charge and shape, cellulose nano-structured materials suspensions display extremely complicated flow characteristics in an aqueous medium. CNCs suspension exhibited lyotropic phase behaviour, whereas CNFs's aqueous showed flocculation characteristics. Upon increasing the shear rate, NCs displayed shear thinning behaviour and eventually aligned themselves along the flow direction. For their application in multiple fields, the lyotropic phase of

CNCs and flocculation of CNF, and their orientation under applied shear-stress are crucial. The prime focus to study the role of CNCs and CNFs as rheology modifiers is because these cellulosic materials are biodegradable, bio-compatible, easily available in bulk, and contain many surface tailorable OH groups.

Numerous researchers have tried to explore the potential of NC in oilfield chemistry, specifically in drilling research on liquid chemistry, oilfield contaminated water treatment and increase in oil recovery (Eichhorn, 2011; Li et al., 2015b; Tingaut et al., 2012). The details of which have been given below.

4.1. Drilling fluids

Rheological characteristics of NC in drilling suspension play an important role in the drilling process (Dai and Zhao, 2019). The incorporation of NC, instead of improving fluid loss and rheology, also enhances the thermal strength of drilling fluid. Li et al. (Li et al., 2015b) compared the potential of microcellulose and S-CNC as rheology modifiers in water-based bentonite slurry. They reported that CNCs based-slurry possesses better rheological characteristics as well as improved thermal strength, thinner mud cake deposition, and lesser water loss. Further, on the addition of polyanionic cellulose to the CNC-containing bentonite mud, the rheological properties of mud, because of the synergistic effect, were noted to be enhanced. In addition, the fluid loss performance of mud was enhanced with the increase in S-CNC concentration. Hall et al. (Hall et al., 2017) utilized the CNFs, CM-CNFs, TO-CNF and cationic CNFs having quaternary amine groups to formulate cement slurries and studied their rheological properties. High-resistance water-based mud was utilized in the shale section of the formation to prevent the shale from collapsing into water. Cationic CNFs, along with quaternary ammonium salt compounds, have been reported to stabilise shale more effectively by preventing water from entering the shale layer and thus lessening the shale expansion. Zhou et al. (Zhou et al., 2023) evaluated the impact of three different nano-materials i.e., CM-CNFs, CM-CNCs and Sul-CNCs on rheology properties

of water/ sodium bentonite-based drilling fluid. A higher shear thinning and viscosity building behaviour was noted for fluids containing CM-CNFs, while CM-CNCs inclusion showed better filtration control and rheology for drilling fluid. Moreover, drilling fluid containing CM-CNCs also exhibited impressive gel strength, salt resistance and thermal strength as compared to CM-CNFs and Sul-CNCs.

4.2. Enhancement of oil recovery

Oil recovery has been enhanced by using NC as emulsion stabilising,
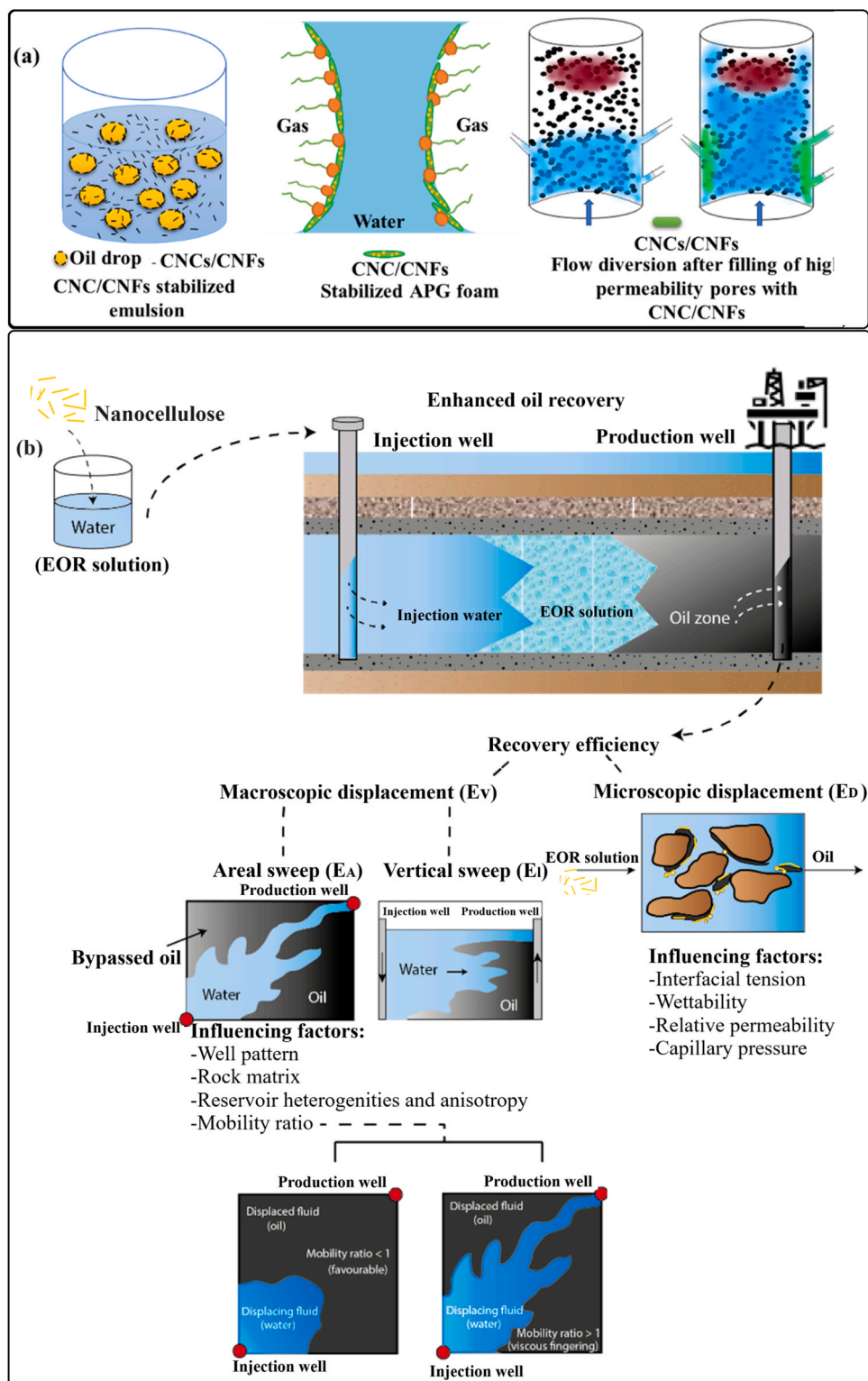
Fig. 4. (a) The mechanistic view of different routes through which oil recovery can be enhanced and (b) illustration of enhanced oil recovery and the overall recovery efficiency [Fig. b reprinted from Ref. (Aadland et al., 2019) under creative common CC BY 4.0 licence]. [Here in Fig. 4b the term Eb quantifies potential of displacing fluid to mobilize the residual oil upon contact; areal sweep (EA) signifies the horizontal area that can be swept and vertical sweep (EI) represents the cross-sectional area that can be invaded].

oil displacing and foam stabilising agents (Fig. 4a). A schematic view of enhanced recovery of oil has been given in Fig. 4b.

4.2.1. Emulsion stabilization

The eco-friendly NC has been widely used to enhance oil recovery as an emulsion stabilising agent (He et al., 2021; Zhu et al., 2021). Their tendency to stabilise emulsions originates from their high aspect ratio and rod-like shape, which results in better adsorption energy (Lu et al., 2021; Tingaut et al., 2012). NC works by adsorbing irreversibly in between the oil-water interface because of its amphiphilic nature, as it contains both hydroxyl groups and hydrophobic C-H moieties. The stabilising process of NC has been categorised into two main theories: first is the adsorption of NC on the oil and water interface, which prevents droplets from aggregating, and second one includes the formation of a stable network (Horozov and Binks, 2006; Xhanari et al., 2011). The hydrophilic or hydrophobic crystal plane of NC turns itself towards the surrounding medium depending upon its hydrophilicity/ hydrophobicity.

To improve the thermal strength as well as the salt-thickening effect of CNFs, a binary mixture of butyl Acrylate (BA) and N, N-dimethylacrylamide (DMA) was graft-copolymerized onto their surface by Liu et al. (Liu et al., 2019). They reported an increase in salinity tolerance (NaCl) from 1 to 8% after surface functionalization. Further, due to enhancements in thermal and salt-thickening behavior, the synthesized CNFs composites have been promised to be a better alternative for petrochemicals for oil recovery applications.

Li et al. (Li et al., 2017) studied the potential of virgin CNFs (carboxyl groups: 0.91 mmol/g) and surface modified [grafted with AMPS (2-acrylamido-2-methylpropane sulfonic acid) and hydrophobic groups] samples CNF-KY (carboxyl groups: 0.91 mmol/g; AMPSS:0.88 mmol/g; and hydrophobic groups: 0.0 mmol/g) and CNF-KYSS (0.91; 0.88; and 0.094 mmol/g, respectively) to enhance oil recovery. CNFs-KYSS showed better salt-tolerance, enhanced stability, and pronounced salt-thickening behavior among different samples. At 0.3 wt%, CNF-KYSS hydrogels reduce the interfacial tension at the crude oil interface and deliver good emulsification. When 0.4 pore volume of CNFs-KYSS fluid slug was injected prior to water flooding, which is done by injecting 4 pore volumes of 1 wt% NaCl, an increase of 6% in original oil in place (OOIP) recovery (with brine, it was noticed to be 45.8%) was noticed. Further, with the CNF-KYSS, the differential temperature also increased to 0.25 MPa; the water cut notably declined from 99 to 93%. Like Li et al., Wen et al. (56) also modified CNFs using AMPS and reported an increase in the thermal stability and the colloidal stability of modified CNFs in sodium chloride solution.

Gestranius et al. (Gestranius et al., 2017) evaluated the stability, droplet size distribution and phase behavior of oil(dodecane)-in-water emulsions stabilised by three different nanocellulosic materials: CNFs, TO-CNFs and CNCs. All samples (0.1–1.5% NC), without using surfactants, formed oil-in-water Pickering emulsions (O/W ratios: 20–35% oil), which rapidly convert into a stable creaming layer. The creaming layer formed by CNFs and TO-CNFs was found to be more stable towards coalescence and high temperature than CNCs. Further, between CNFs and TO-CNFs, later one forms a stable dispersion of oil droplets beneath the creamy layer, suggesting that high charge density plays a crucial role in electrostatic interactions. Recently, sodium 3-chloro-2-hydroxypropanesulfonate functionalized CNCs along with nonionic surfactants (APG1214), have been used to enhance oil recovery in low permeability reservoirs (Z. Li et al., 2023a,2023b). The surface functionalized CNCs showed better dispersion than virgin CNCs because of the presence of hydrophilic sulfonic acid groups on their surface. Further, when blended with nonionic surfactant to form a flooding system, due to the synergistic impact of the combined system, the resultant system showed low (0.03 mN/m) oil - water interfacial tension, higher emulsification stability and a better tendency to change the oil-wetting surface to water-wetting. The combined system also increased (20.2%) the oil recovery with a low permeability of 30.13×10^{-3} μm^2.

Parajuli et al. (Parajuli et al., 2020) enhanced the biodegradation of crude oil by increasing the oil/water interface area using surfactant-free CNCs dispersion. When studying the biodegradation of C_{15}-C_{20} hydrocarbons using gram-negative bacillus, after incubation for 5 days, the extent of biodegradation was noted to enhance from 1–12 to 6–19%. Their results depicted that physico-chemical properties/concentration of CNCs, divalent ions and salinity play a significant role in the biodegradability/stability of emulsions. On evaluation of impact of concentration of CNCs (varied from 0.4 to 1.0 wt%) on stability of the crude oil emulsion in brine (5:95 v/v%) in synthetic water, API brine and sodium chloride solutions, it was noted that when CNC concentration was > 0.8 wt%, the degree of coalescence was higher in API brine (ionic strength 1.9 M); whereas it was minimum in synthetic water (0.65 M). Further, no coalescence was noted for NaCl solutions of different ionic strengths (0.32–1.9 M). Kinara and Pal (Kinra and Pal, 2023)varied the amount of CNC (1.03–7.41 wt%) for stabilising the emulsion of oil of varying concentrations 10–70 wt%. After the addition of CNCs, better stability of the emulsion with respect to coalescence and creaming was noted. The emulsion showed non-newtonian flow, and an increase in consistency index and a decrement in viscosity index with an increase in either an CNCs or oil concentration was reported (Fig. 5).

From the above discussion, we can conclude that the charge on the surface of NC controls the electrostatic repulsion between the droplets, inhibits the droplets from coalescing, and thus enhances the emulsion stability.

4.2.2. Foam stabilization

The stability of the foam has a significant impact on its potential to improve oil recovery. According to reports, crude oil drops destabilise foam films in three ways during the oil recovery process: by interconnecting the surfaces of two films, disrupting surfactant orientation at the interface, and squeezing out film liquid (Karakashev and Grozdanova, 2012). Wei et al. (Wei et al., 2018)stabilized the surfactant foam by utilizing surface functionalized CNF and then used the foam system in the foam oil recovery process (Fig. 6a). The synergistic impact of CNFs and surfactant was studied by evaluating the oil/water/solid interface, foam decaying behaviour and its morphology, interfacial rheological behavior, etc. After incorporating functionalized CNFs in surfactant solutions, a decrement in the oil/water interfacial tension was noted; however, a counter impact was seen on the wettability and emulsifiability of the surfactant. Further, the surfactant foam's thickness was remarkably enhanced and liquid drainage was hindered after the addition of CNFs. It has been confirmed using a microscopic visualisation model that functionalized CNFs offer the foam membrane good stability during migration in porous media and result in a noticeable decrement in the residual oil saturation. Furthermore, an increase in oil recovery was observed because of the leftover oil from the water flooding.

In another study, Wei et al. (Wei et al., 2019) used lignin-containing CNFs along with surfactant for stabilizing the interface of liquid foam and reported five times better stability of foams when compared to surfactant alone (Fig. 6b). This higher stability has been attributed to the development of an elastic interface for foams because of the hydrophobic interaction between lignin-containing CNFs and surfactant, which hinders the probability of coalescence and drainage. The foams offer excellent choices for effective oil recovery processes because of their elastic interface, which gives them great mobility control.

4.2.3. Oil displacing agents

Several researchers have also utilized NC as an oil-displacing agent to enhance oil recovery (Aadland et al., 2019; Liu et al., 2019). Molnes et al. (Molnes et al., 2018) used flooded CNC, dispersed in low salinity (LS) brine (CNC-LS), on highly porous sandstone cores to enhance the oil recovery. They validated that most of the CNC particles could penetrate through cores at 60, 90, and 120 °C. Additionally, when CNC-low salinity brine was used in tertiary mode during oil recovery, the oil recovery was seen to increase at both 60 °C (45.8% (with LS) to 51% (with
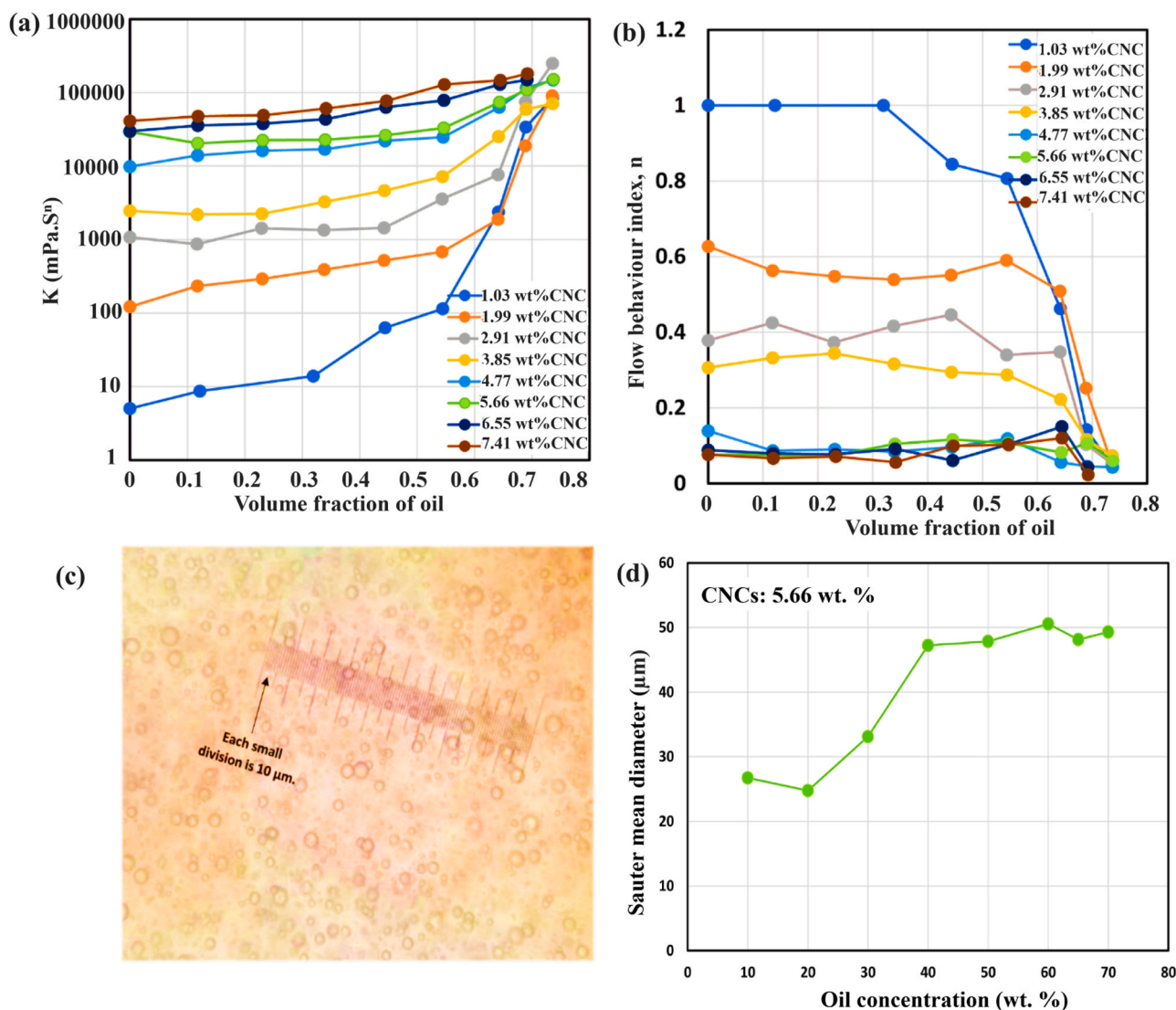
Fig. 5. Comparison of (a) consistency index (k) and (b) flow behavior index (n) of O/W emulsions thickened and stabilized with varying amount of CNCs. (c) phoyomicropgraph image of O/W emulsion stabilized by CNCs and (d) impact of oil concentration on Sauter mean diameter at fixed concentration i.e., 5.66 wt% of nanocrystalline cellulose.

"Reprinted from Ref. (Kinra and Pal, 2023) under creative common CC BY 4.0 licence".

CNC-LS) and 90 °C (66 to 69.4%), indicating that CNCs-LS have a significant potential to be used for utilisation in oil recovery. A good injectability for CNC into sandstone has been noticed when CNC concentration varied from 0.5 to 2 wt% and through viscosity measurement, it has been confirmed that CNC particles moved through the pores without any adsorption. Kusanagi et al. (Kusanagi et al., 2015), after flooding the sandstone core with API brine, carried out gel treatment by injecting CNFs suspension and AlCl$_3$ cross-linkers successively to block the high permeability zone. The gel treatment increased oil recovery from 13.3% to 24.3%.

Raza and Gates (Raza and Gates, 2021) flooded 1 and 2 wt% of CNC nanofluids prepared in deionized water to recover oil from a minor gap in the Hele-Shaw cell. Comparing the outcomes, they discovered that CNC nanofluids form a stable interface and significantly boost oil recovery (up to 98%) at higher concentrations (2 wt%). Through microscopic investigation, it has been confirmed that nanofluid forms a microemulsion along the interface in the oil stream after passing through the oil phase. This further reduces the effective interfacial tension and causes the oil phase to be engulfed and mobilised. The above finding may be pretty helpful in enhancing oil recovery from fractured

surfaces. Wani et al. (Wani et al., 2020) used CNCs as fluid-diverting agents to improve oil recovery. Fluid diverting agents are generally used to block the high permeable zone so that injecting fluid may come in contact with a less permeable oil-containing zone and enhance oil recovery (Fig. 7). While using this green technology, they reported that CNC agglomeration remains stable at high temperatures as well as at higher salt concentration. From above discussion, we can see that numerous factors such as salt concentration, surfactant or electrolytes, shear stress, shear strain, etc., affect the overall rheology of NC-based suspension. So, in this manuscript, we will focus on exploring these factors.

5. Factors impacting the rheological properties of nanocellulose suspension

NC gels show shear thinning characteristics and thixotropic behaviors. Enhancement in the concentration of NC and ionic strength leads to the development of higher network strength. To tune the rheology of NC for various processing in multiple fields is of prime interest nowadays. The numerous factors which affect the rheological properties of an
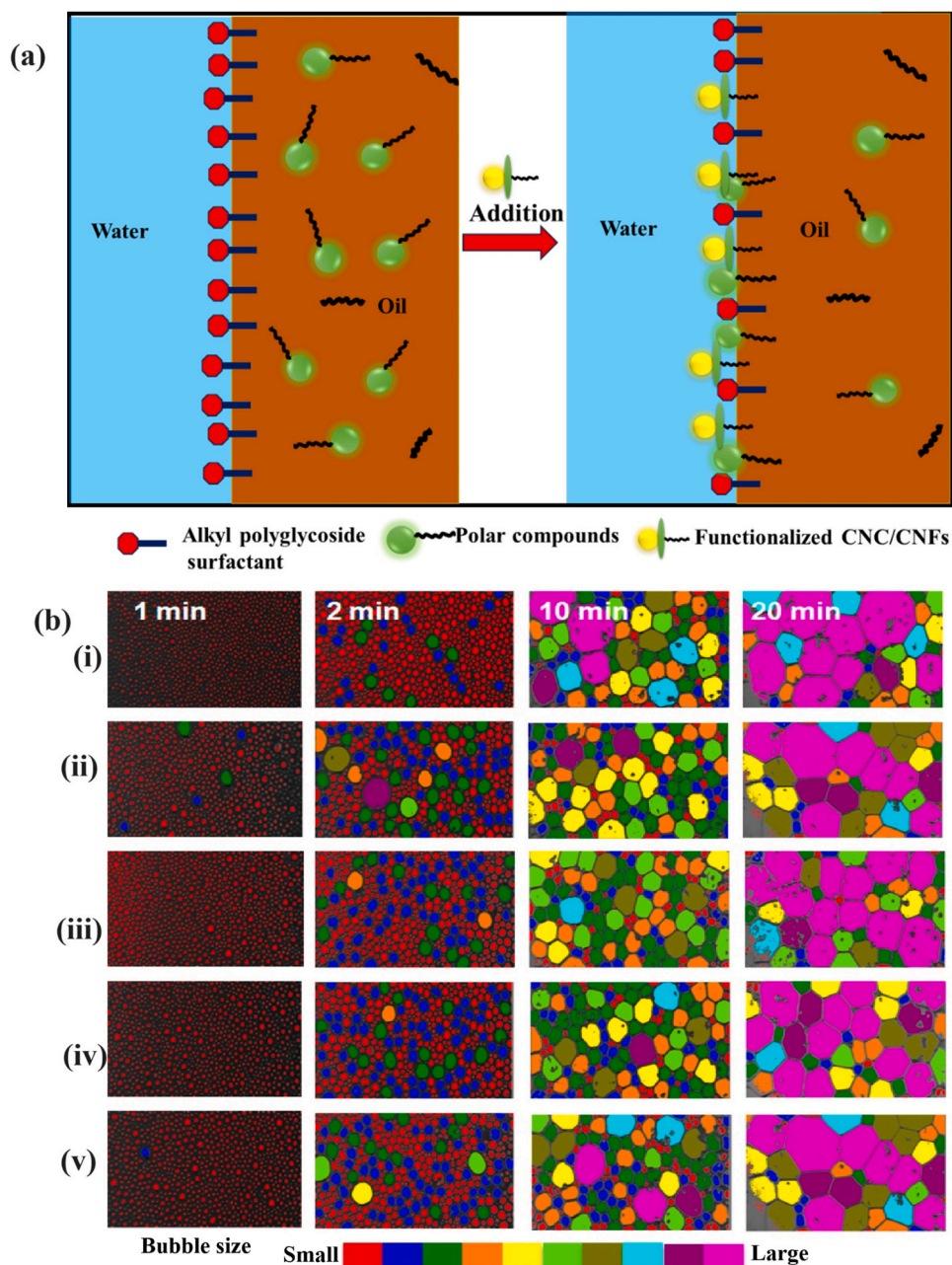
Fig. 6. (a) Schematic view of the interface interactions (Adapted with permission from Ref. Wei et al., 2018) and (b) images of different foam bubbles with time: (a) surfactant-only, lignin containing CNFs (b) sample 1 (containing 15.5 wt% lignin), (c) sample 2 (containing 11.7 wt% lignin), (d) sample 3 (containing 8.66 wt% lignin), and (e) sample 4 (containing 4.79 wt% lignin).
"Reprinted with permission from Ref. (Wei et al., 2018), Copyright 2019, ACS."

aqueous suspension of NC have been explored below. The impact of surface functionalization of NCs and their aspect ratio on the rheology of NC suspensions have already been thoroughly discussed in our previous review article(Rana and Thakur, 2023), so here just a superfacial idea was given.

5.1. Instrumental factors

The instrumental factors like the type of rotational rheometer and shear rate strongly impact the rheological properties of NCs suspension.

The commonly used geometries of rotational rheometer for measuring the viscosities of NC suspensions are displayed in Table 1 (Biliuta et al., 2023b; Cainglet et al., 2023; Guo et al., 2023; Yamagata et al., 2022). Some suspensions showed contradictory behaviour due to

the wall depletion effect when the gap between the parallel plates is reduced. Thus, some other factors, such as gap-dependent floc and geometrical constraint, should be considered, especially for thick fibrils (Hubbe et al., 2017; Li et al., 2021). Mostly, continuous shearing of fibrous suspension in a rheometer having smooth geometry leads to heterogeneous flows (e.g., shear banding and wall depletion) (Nechy-porchuk et al., 2014; Saarikoski et al., 2012; Saarinen et al., 2009; Schenker et al., 2018; Vadodaria et al., 2018). Wall depletion becomes a severe issue when one wants to quantify the rheological characteristics of fibrils in suspension. Since fibrils or particles become depleted at the flow or measurement device boundaries at a simple shear flow rate, this phenomenon leads to a much lower viscosity than bulk viscosity. Various forces such as chemical, gravitational, viscoelastic, hydrody-namic and steric have been reported to act upon dispersed phase fibrils
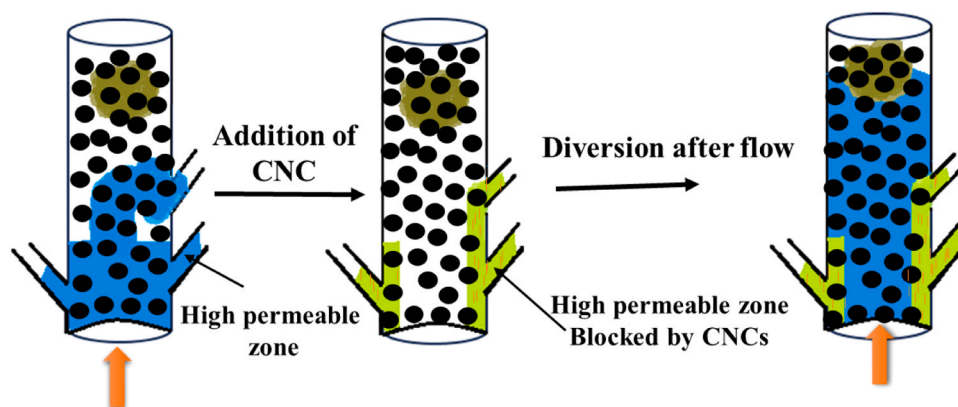
Fig. 7. Showing how CNC addition blocked the highly permeable pores. (Adapted with permission from Ref. Wani et al., 2020).".

adjacent to smooth boundaries (Barnes, 1995; Hubbe et al., 2017).

The wall depletion effect may further lead to shear banding instead of loading under the same shear rate, resulting in the generation of the depleted and thickened regions in a rheometer, more specifically in a couette (concentric cylinder)-type viscometer apparatus (Hubbe et al., 2017; Ovarlez et al., 2009). Such instabilities in flow may lead to false data while measuring the rheological characteristics. Further, depleted areas are not only present at the walls, but their presence may be expected at other points in a sheared NC suspension. A couple of researchers have reported the presence of wall depletion and band formation in nano cellulose suspension in the gap between the wall and the rotating cylinder (Barnes, 1995; Hubbe et al., 2017; Lerouge and Olmsted, 2020, 2020; Martoïa et al., 2015; Nazari et al., 2016).

The concentric vane or serrated plate viscometers are good options to reduce or minimize the wall depletion effect, as they produce authentic values of G′ and viscosity (Naderi and Lindström, 2016; Nechyporchuk et al., 2016b, 2014; Rezayati Charani et al., 2013). On the other hand, in a bucket vane viscometer with a wide gap, low stress at the cup edge prevents the fibrils from slippage, whereas high pressure near the vane edge results in good contact with the fibrils (Mohtaschemi et al., 2014). Further efforts were also made to eliminate the wall depletion effect by introducing the profiled surface in a concentric cylinder, leading to substantially better measurements of both moduli and viscosity for 2 wt % CM-CNF suspensions (Nechyporchuk et al., 2015). When different types of viscometers, such as smooth cone-plate, serrated concentric cylinder and serrated cone-plate, were compared for their efficiency in studying the rheology of TO-CNF suspension, it was found that serrated concentric cylinder gave the most authentic results (Mondal, 2015).

Wall slip impacts for three different CNFs systems, namely enzymatically pretreated, CMC grafted and CM-CNFs, were evaluated using smooth and serrated metal concentric cylinder (bob and cup) geometries. It has been noticed that the rheological characteristics of CM-CNFs are slightly impacted by wall milling. However, unstable Enz-CNFs and CMC-grafted CNFs displayed a considerable degree of ball-milling impact (Naderi and Lindström, 2016). Using a double wall concentric cylinder may be a viable way to lessen the wall slip effect. Still, it has the drawback of only being appropriate for small viscosity samples (Jowkarderis, 2016; Zhu and De Kee, 2008).

Shear thinning behaviour has been observed for both CNF and CNCs suspensions(Li et al., 2015a; Shin and Hyun, 2021; Tang et al., 2018) with increase in shear rate. The viscosity of CNF's suspension was evaluated as a function of the amount of carboxyl contents (varied from 0.01 to 1.14 mmol/g) as well as wt% of CNFs (0.25 to 1.5 wt%). At lower carboxyl contents (0.01 mmol/g), the CNFs exhibited a decrease in viscosity with an increase in the shear rate in all three regions. In region I, viscosity decreases sharply due to the better dispersion, breakdown and orientation of low carboxylated CNFs (Shin and Hyun, 2021). In region II, i.e., at the intermediate shear rates, a

continuous/sharp decrease in viscosity was prohibited because more entangled CNF flocs were generated.

Further, a sharp decrease in viscosity, i.e., severe shear thinning behaviour, was observed in region III. This behaviour has been related to the breakdown of entangled flocs and their orientation in the shear direction. Similar behaviour was observed for highly carboxylated CNFs samples (0.66–1.14 mmol/g); however, in these samples, no sharp shear thinning behavior has been observed at the region I, i.e., at low shear rate. This might be because of the poor dispersion of CNFs because of high carboxyl contents on CNF's surface.
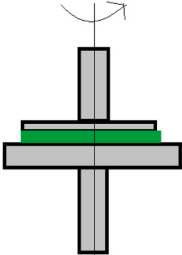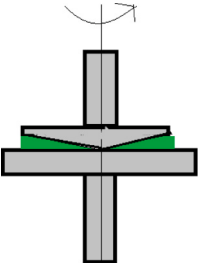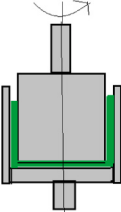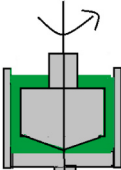
Further, when the amount of CNFs was varied from 0.25 to 1.5 wt%, shear thinning behavior was observed to take place in three regions. In regions I and III, a continuous decrease in viscosity was observed because of the breakdown of CNFs flocs and their orientation and disintegration of highly entangled complex flocs and orientation of disintegrated flocs along the shear direction, respectively. However, no sharp decrease in viscosity was observed in region II due to the complex network formation between flocs. Further, in the case of UN-CNF, in addition to three regions, as described above for carboxylated CNFs, the fourth region at a much higher shear rate was also observed, where the viscosity was noticed to be almost independent of the shear rate because of the complete disintegration and orientation of entangled flocs (Li et al., 2015a) (Fig. 8a).

The Sul-CNCs (Fig. 8b) exhibited the characteristic of an isotropic suspension at very low concentration (1 wt%), i.e., showed shear thinning behaviour at lower shear rates, and Newtonian plateau at intermediate or high shear rates (Tang et al., 2018). However, at 2 wt% suspension or for cationically (glycidyltrimethylammonium chloride) modified CNCs (1 and 2 wt%), a three-region shear thinning behavior was observed, which includes shear-thinning at a low shear rate, shear thickening at intermediate and shear thinning at higher shear rates. This behaviour has been attributed to the gel-like characteristics of the highly entangled networks of the rigid CNCs. Contrary to the above results, in another study, Sul-CNCs suspension at low concentration, i.e., dilute concentration (1 and 3 wt%) displayed Newtonian plateau at both low and high shear rates; however, at intermediate shear rates, it showed a shear thinning behavior (Shafiei-Sabet et al., 2014). Further, at the semi-dilute regime, similar to cationically modified CNCs (Fig. 8b), three regions were observed in viscosity vs. shear curves, i.e., shear-thinning region at low, a plateau at intermediate and again a shear-thinning region at high shear rates. At very high Sul-CNCs concentrations (12 and 15 wt%), only a single shear-thinning region was noticed for CNC suspension.

5.2. Inner factors
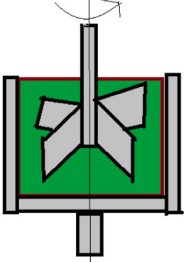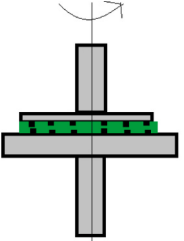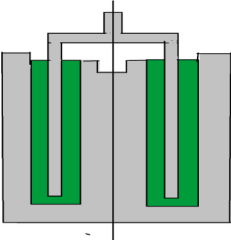
The zeta potential value and crowding factors of NCs are the two main internal factors impacting the suspension rheology. The zeta-

Table 1

Showing the different rheometers, which have been utilized to measure the NC rheology, their benefits and drawbacks.

Type of Geometry of Rotational Rheometers	Benefits	Drawbacks	References
Parallel plate geometry **Parallel Plate**	Utilized for measuring NC small volume samples having intermediate to high viscosity	Contradictory to the wall depletion effects, here, G′ increases progressively with a decrement in measurement gap, resulting decline in viscosity.	(Barnes, 1995; Kim et al., 2023; Qi et al., 2023; Saarikoski et al., 2012; Vadodaria et al., 2018; Xu et al., 2024; Yamagata et al., 2022)
Cone and plate geometry **Cone and Plate**	Measure small volume samples having viscosity varying from intermediate to high	The particle/fibril size should be < 10% of the gap height between the bottom plate and the truncated cone. Since in this kind of geometry, when particle size is more or when the gap near the tip of the cone is very small, then the mobility of CNFs is constrained more profoundly, and thus, it may lead to a higher G′ for UN-CNF suspensions	(Ilyin et al., 2023; Saarinen et al., 2009)
Concentric Cylinder geometry **Concentric Cylinder** , **Concentric Cylinder**	Possess less sensitivity to particle settling and solvent evaporation effects. But one has to ensure that geometry of appropriate size and appropriate gap size has been maintained	Measure the viscosities of larger sample volumes having low viscosity	(Cainglet et al., 2023; Koppolu et al., 2022; Z.Li et al., 2023a,2023b;Saarinen et al., 2009)

Table 1 (*continued*)

Type of Geometry of Rotational Rheometers	Benefits	Drawbacks	References
Concentric vane geometry	Reduces wall effect	Give more accurate values of G′ and viscosity	(Beugre and Gnagne, 2022; Mohtaschemi et al., 2014)

Vane Concentric

Serrated Plate geometry	Reduces wall effect	Give more accurate values of G′ and viscosity	(Mondal, 2015; Rissanen et al., 2021)

Serrated Plate

Double wall concentric cylinder geometry	Greatly reduces the wall slip impact. Give real yield stress results.	Used for low viscosity samples	(Jowkarderis, 2016; Zhu and De Kee, 2008)

potential measurement provides information about the type and density of charged groups present on the surface of the particles. It is a good indicator of the stability of NC suspension, which depends on the electrostatic repulsive forces between the charged groups present on CNCs or CNFs particles/fibers. The zeta-potential value of CNC/CNFs suspensions gave an insight into the tendency of CNCs or CNFs to agglomerate or form flocs. The Zeta potential value depends upon the type of extraction/synthesis/surface modification techniques employed as well as the dimensions of NCs (Beyene et al., 2018; Liang et al., 2021). Beyene et al. (Beyene et al., 2018) reported a zeta potential value of -40.5 ± 2.5 to -43.8 ± 0.8 mV and -38.9 ± 2.7 to -42.6 ± 3.5 mV for CNCs, extracted from filter paper and wood pulp, respectively, by utilizing enzymatic treatment followed by acid hydrolysis. Generally, any value $\geq +30$ mV of ≤ -30 mV (minimum threshold) confirms the electrostatic stability, i.e. better electrostatic repulsion between charged particles and thus better dispersion. However, it is always not so, since at values $\geq +30$ mV and ≤ -30 mV the long-range strong van der Waals interactions may lead them to agglomerate, specifically in the case of CNFs. Further, any suspension with a value of 0 to ± 5 mV flocculates rapidly.

Various researchers have studied the Zeta potential value of NCs. A zeta potential value of -15 mV was reported for NCs (cellulose nanowhiskers) extracted from cotton fibres using microbial hydrolysis technique (Satyamurthy et al., 2011), ranging from -25 to -31 mV for CNFs extracted from cotton fibers utilizing sulphuric acid for hydrolysis (de Morais Teixeira et al., 2010), -30 to -82 mV for CNFs synthesized through mechanical grinding of carboxymethylated pulp suspension (Shin and Hyun, 2021), -31 mV for CNCs synthesized from recycled paper using enzymatic treatment (Filson et al., 2009), in the range -52 to -58 mV for CNCs synthesized from filter paper through sulphuric acid hydrolysis (Boluk and Danumah, 2014), -30.70 to -35.9 MV for CNCs synthesized by employing sulphuric acid treatment to kraft pulp followed by ultrasonication (Shafiei-Sabet et al., 2012), -35.4 ± 2.0 mV for CNCs extracted from microfibrilled cellulose using sulphuric acid cum homogenization treatment (Li et al., 2015b), and -16 to -27 mV for CNCs extracted from microsrytalline cellulose using sulphuric acid hydrolysis (Prathapan et al., 2016). Fig. 9(a) shows how zeta potential value impacts the stability of colloidal suspension of no oxidated CNFs (NCNF), low oxidated CNF (LCNF) and high oxidated CNFs (HCNF) (Liang et al., 2021). Among various samples, HCNF demonstrated maximum zeta potential (>-30 mV) values and thus better stability; however, other samples, i.e., NCNF and LCNF, showed poor stability because of Zeta potential value < -30 mV.

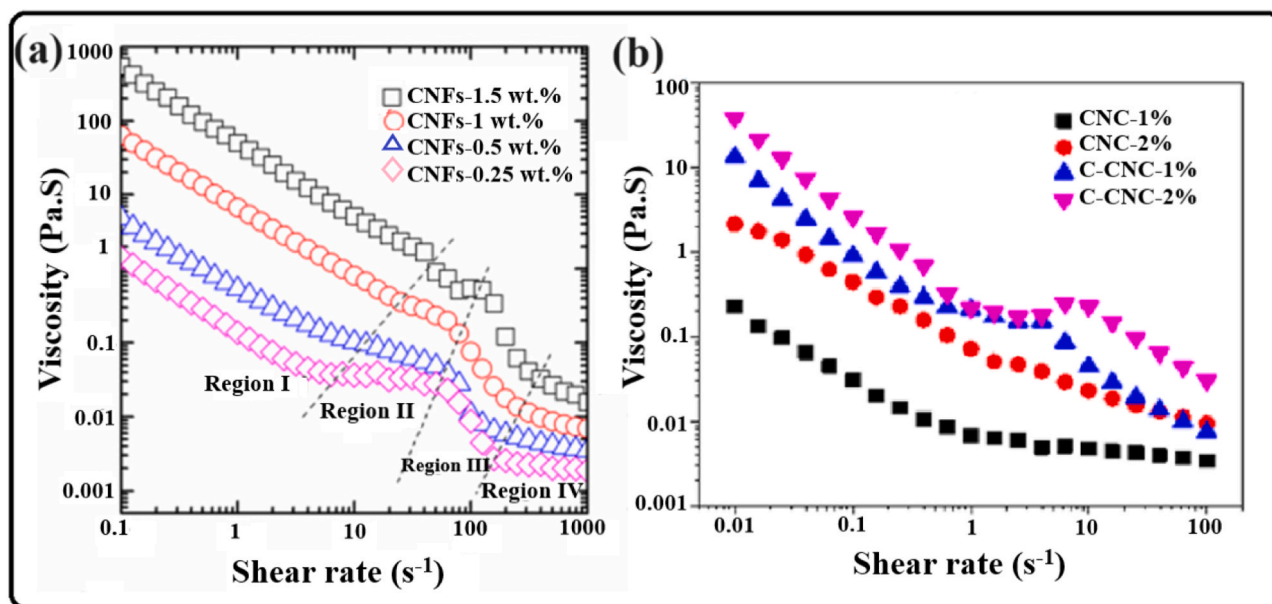Geng et al. (2018) found an increase in viscosity of CNFs suspension

Fig. 8. Impact of concentration of (a) UN-CNFs on shear thinning behavior of suspensions (Li et al., 2015a). ; and (b) cationically modified CNCs (C-CNCs) on shear thinning behavior (Tang et al., 2018).
(a) Copyright {2015} American Chemical Society."]"Reprinted with permission from reference (Li et al., 2015a). (b) [Reprinted from Ref. (Tang et al., 2018) under creative common CC BY 4.0 licence

(0.05 wt%) with an increase in charge density from 320 to 820 μmol/g because of better fibrillation of CNFs at low charge density promoted by the repulsion among similar charged CNFs; however beyond that a gradual decrease in viscosity was noticed. The decrease in viscosity has been attributed to lower agglomeration of fibers due to higher repulsive forces among CNFs.

Lee et al. (Lee et al., 2021) reported that the zeta potential value of CNCs increases gradually with high pressure homogenization cycles because of exposure of more and more sulfate half ester group. They demonstrated a zeta potential value ranging from -34.6 to -98.7, -31.0 to -84.0 and -37.4 to -45.4 mV for CNCs suspension extracted from MCC, softwood pulp (SP) and cotton pulp (CP), respectively [Fig. 9(b)]. Further, a strong correlation between zeta potential value and turbidity was noted for CNCs samples. With an increase in zeta potential value, an increase in turbidity was observed. All aforementioned results confirm how surface chemistry and the presence of hydrophilic or hydrophobic groups onto CNCs/CNFs surface controls the zeta potential value and, thus, overall stability of NC suspension.

The rheological properties of NCs in aqueous suspensions can be well studied by evaluating the crowding factor (N), which is a function of concentration and aspect ratio of NC in suspension. The flocculation of CNFs in an aqueous system depends upon the value of N. Proposed by Kerekes.

and Schell (Kerekes and Schell, 1992) and further extended by Kropholler et al. (Kropholler and Sampson, 2001), the following equation can used for calculating the $N_{corrected}$ (N′) for the CNFs.

$$N^{'} = \frac{2}{3}\varnothing\left(\frac{l}{d}\right)^{2}\left(1+CV^{2}\right)^{4}$$

Here l is the length of fibers; d is the diameter;$\varnothing$ is the concentration of CNFs in the system; CV coefficient of variation is calculated as per the protocol given by Kropholler et al. (Kropholler and Sampson, 2001).

Geng et al. (Geng et al., 2018) reported N′ values ranging from 20 to 107 for CNFs, when concentration and charge density was varied from 0.01- 0.3 wt% and 380–1360 μmol/g, respectively. The variation of viscosity, storage modulus, loss modulus with concentration of CNFs (having charge density: 380 μmol/g) is given in Fig. 10a. The observed

behavior was beautifully described by the crowding factor. When N′ was <16 (gel crowding factor), fluid-like behavior was observed (Newtonian behavior); however, when $16 < N^{'} < 60$, viscoelastic behavior with shear thinning characteristics was reported (Non-Newtonian behavior). During the regime $16 < N^{'} < 60$, a slope of 2.3 (approx) was noticed by a couple of researchers (Naderi et al., 2014b, 2015b). Further, the above behavior was also affirmed through dynamic rheological study. When N′ value was lower than the 16, loss factor (tanδ) [which is the ratio of loss modulus (G'') and storage modulus (G′)], the value lies <1, confirming the fluid-like behavior at N′ <16. However, at N′ $=16$, the loss factor value was found to be 1, demonstrating the gel formation tendency of suspension. Beyond N′ >16, the loss factor value was found to be >1 (since G′>G''), confirming the solid-like behavior of suspension. Further, when N >60, CNF suspension showed truly gel characteristics, having G′ much higher than G'' (Naderi et al., 2014b, 2015b).

Wang et al. (Wang et al., 2019), contrary to the above results, reported slightly lower gel crowding factor values for low as well as highly charged TO-CNFs (N′=14). Such variation in value has been attributed to discrepancies in the pretreatment, which might result in CNFs of unequal dimensions, different crystallinity, and flexibility. Further, they reported a slightly higher slope (in the range 2.8 to 3.2) when the concentration of highly charged CNFs (3.9–39.4) was varied from 0.1 to 1.0 mg/ml. The rheological behavior of CNFs in aqueous suspension has been divided into dilute (having N′<14) and semi-dilute (N′>14) concentrated regimes. Thus, the transformation of CNFs suspension from dilute to semidilute and to further network region can be best described by the concept of the crowding factor. In the dilute regime, fibers can rotate and move freely; in the dilute region fibers undergoes interaction and entanglement, while in the network region fibers are completely or partially immobilized. It can be concluded that the crowding factor considers the impacts of CNFs surface charge, while no impact of ionic strength was noted. The phase diagrams for CNCs suspension in aqueous medium against concentration were given by Parker et al. (Parker et al., 2018) and Xu et al. (Xu et al., 2019) (Fig. 10b). Change in CNC phase, in addition to concentration and aspect ratio, has been influenced by other factors such as zeta potential value, ionic strength and other colloid characteristics.
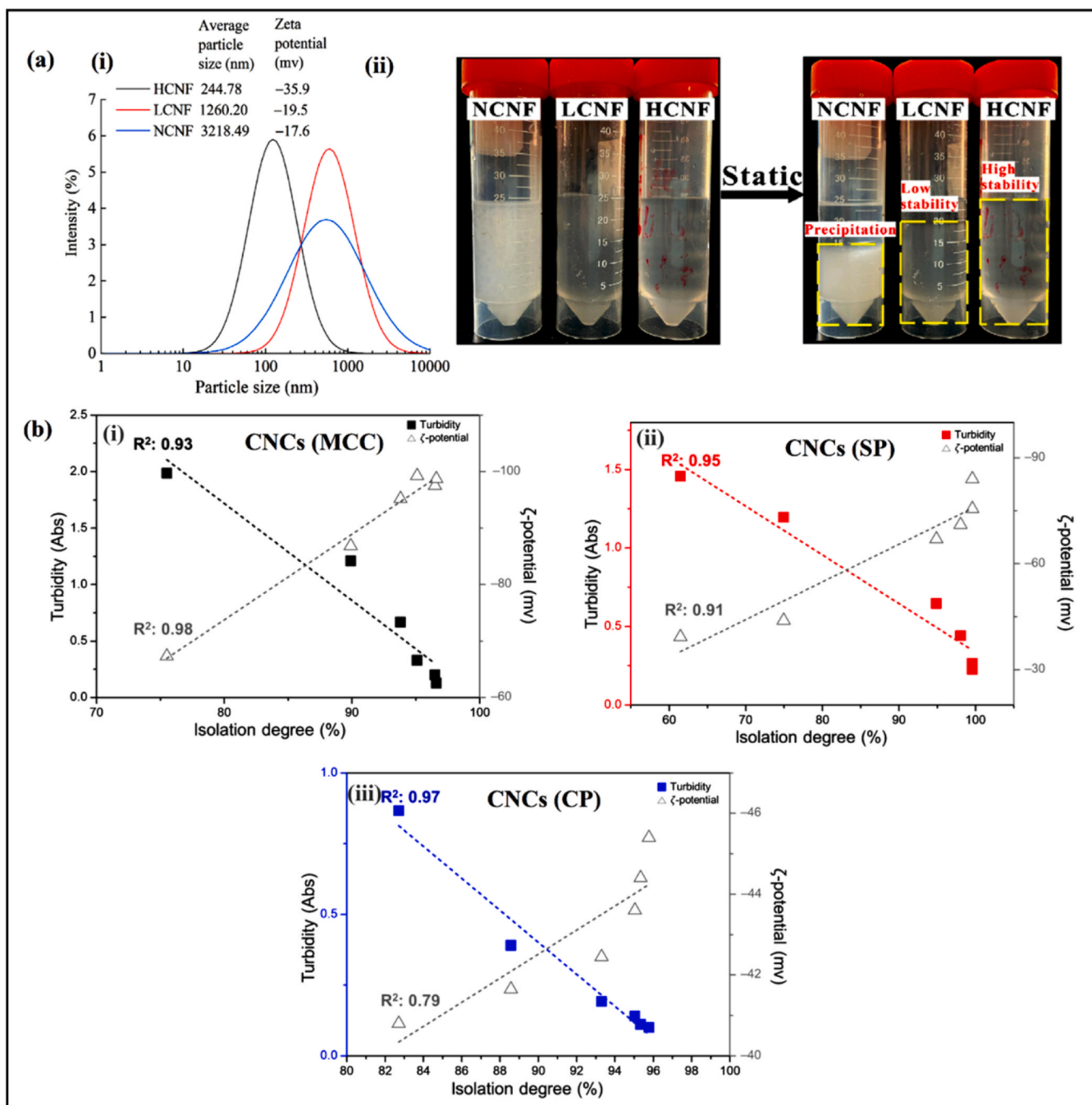
Fig. 9. (a) (i) Zeta potential value and particle size distribution and (ii) stability of CNF suspensions (Liang et al., 2021) (b) a comparative view of zeta potential value and turbidity of CNCs suspension (Lee et al., 2021)
(a) [Reprinted from Ref. (Liang et al., 2021), Copyright 2021, RSC, under CC BY]. (b) [Reprinted from Ref. (Lee et al., 2020), Copyright 2021, MDPI, under creative common CC BY 4.0 licence].

5.3. Environmental factors

The various environmental factors that have played a crucial role in the overall rheology of NCs suspensions are temperature, pH, time and magnetic/electrical properties. The details of which have been discussed below. Change in the microstructure of the NC suspension with temperature directly impacts its rheological behavior. To evaluate the temperature impact, steady shear viscosity is generally measured at different temperatures for samples at various NC concentrations. It has been observed that at very low CNCs suspension (3 wt%), viscosity declines with an increase in temperature at all shear rates (Shafiei-Sabet

et al., 2012) (Fig. 10c-f). This behavior has been attributed to a small amount of ordered domains leading to isotropic nature. However, at higher 5 or 7 wt% CNCs suspension, the suspension becomes predominately anisotropic showing three region behavior. A decrease in viscosity in regions I and III at all temperatures (10–50 °C) has been observed; however, in region II, at the intermediate state, the viscosity was found to be almost the same. On comparing the viscosity of samples in region I, a sharp increase in viscosity has been noticed at 40 °C. Further, at 10 wt% CNC concentration, viscosity was found to be independent of temperature in the range of 10–40 °C, but beyond that, a sharp increase in viscosity was observed. During the analysis of change
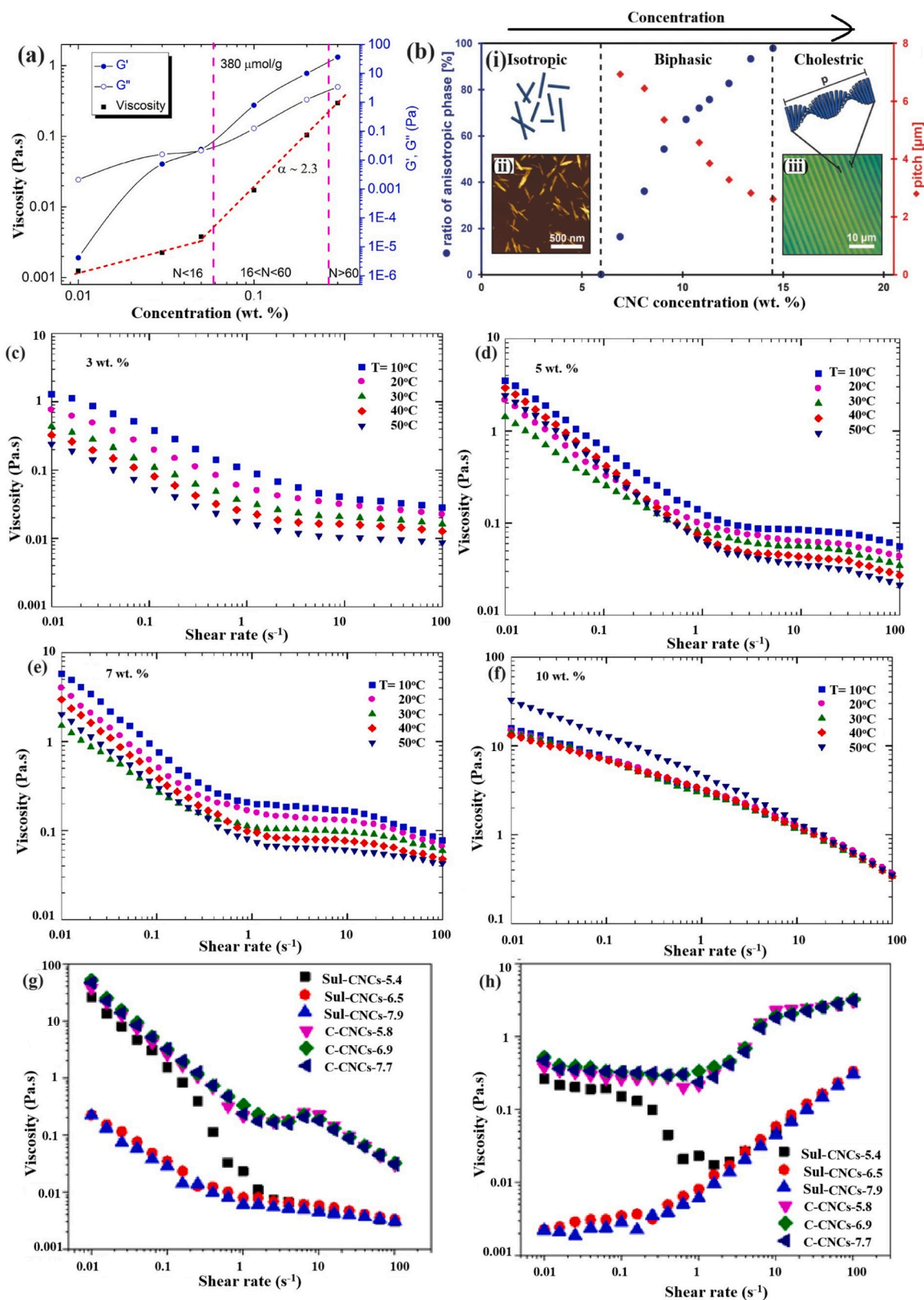
Fig. 10. (a) Steady shear viscosity at 100 s^{-1} and dynamic rheological properties at 1.0 Hz of CNF suspensions (380 μmol/g) as a function of concentration (Geng et al., 2018). [Reprinted from Ref. (Geng et al., 2018), Copyright 2018, ACS, under CC BY], (b) Self-assembly of CNC with increase in concentration (Parker et al., 2018). Copyright {2012} ACS.", and (g) Viscosity and (h) Shear stress as a function of shear rate for Sul-CNCs and C-CNCs suspensions at various pH (Tang et al., 2018). "Reprinted from Ref. (Tang et al., 2018) Copyright 2018, MDPI, under Creative Common CC BY 4.0 license".
(a) Reproduced with permission from Wiley under CC-BY license, steady shear viscosity vs shear rate at different temperatures (10 to 50 °C) for various CNCs concentrated suspensions (c) 3 wt%, (d) 5 wt%, (e) 7 wt%, and (f) 10 wt% (Shafiei-Sabet et al., 2012). (b) "Reprinted with permission from reference (Shafiei-Sabet et al., 2012).

in complex viscosity with temperature for different CNC suspensions (3, 5, 7, and 10 wt%), it has been demonstrated that at low concentration (3 wt%), the complex viscosity declines continuously with temperature, however, at higher CNCs concentrations the decrease in complex viscosity was observed up to certain critical value, and beyond the critical values, the viscosity was noticed to be increased. The critical values for 5, 7 and 10 wt% CNC suspension was noticed to be 42, 36 and 27 °C, respectively. In addition to concentration, the shear rate also significantly impacts the microstructure of CNC or Sul-CNC suspension, causing different temperature-dependent flow behavior. In another study(Tang et al., 2018), at a very low concentration of 0.5 wt%, CNC and cationically modified CNCs, irrespective of temperature (varied from 25–45 °C), displayed pseudo plastics and three region behavior, respectively. Both samples showed decreasing trend in viscosity with increase in temperature; however, CNC shear thinning behavior was observed over the whole shear range whereas for CCNC suspensions mixed trend was observed (a small increase in viscosity was also observed at mid of curve). Further for enzymatically pretreated (Lowys et al., 2001; Pääkkö et al., 2007) and microfluidizer fibrillated and mechanically fibrillated CNFs, no significant impact of temperature on the dynamic moduli of CNFs was noted (tested in the range of 20–80 °C, and 25–60 °C, respectively). With an enhancement in temperature, a slight increase in CNFs network was demonstrated.

On varying the pH values below and above pKa (i.e., the negative decadic logarithm of the acid dissociation constant), the rheology of NC suspension was noticed to be dramatically changed due to protonation and deprotonation of surface functional groups present on NC, as well as by counter ion effects. pH over pKa causes the deprotonation of surface functional groups, which strongly induces electrical double-layer repulsion and creates a weaker network. However, when pH falls below the pKa, protonation of functional groups occurs, which in turn makes the attraction forces more powerful. Thus, contrary to pH above pKa, it creates a tighter network. The pKa values depend upon the type of functional group present on the NC surface. For example, sulphate and carboxyl groups' values lie in the range − 3 and 3–4, respectively. Further, the counter ion effect can also be noticed by using hydrochloric acid or sodium hydroxide to change the pH of the suspension.

Since for sulfate groups, pKa values lies in the negative, therefore Sul-CNC will be in its deprotonated form in aqueous suspension. Fig. 10 (g, h) displays the steady shear viscosity of Sul-CNC and catatonically (glycidyltrimethylammonium chloride) modified CNC (C-CNC) at various pH values maintained by using NaOH (Tang et al., 2018). The shear viscosity was noticed to increase with a decrease in pH from 7.9 to 6.5 and 5.4 in the case of Sul-CNC. Such behaviour has been ascribed to the screening of electrical double-layer repulsion with a decrease in pH values. However, for catatonically modified Sul-CNC, no such variation was observed because of the absence of a negative charge on the surface, making it insensitive to pH variations. Further, for cationically modified CNC, the viscosity of resulted suspensions was found to be higher than that of Sul-CNC suspension. It clearly indicates that quaternary ammonium salt remains intact under the impact of varying pH. Qi et al. (Qi et al., 2019) reported higher viscosity for Sul-CNC suspension in acidic (pH: 4.78) or basic conditions (pH:9) than in neutral conditions. These results might be because of the extensive aggregation of Sul-CNC upon the addition of HCl or NaOH. This result is probably caused by the addition of H^+ or $Na^{+,}$ which led to the protonation of Sul-CNC and extensive CNC aggregation in the system. Xu et al. (Xu et al., 2017) reported a continuous increase in the viscosity of Sul-CNC suspension when pH was varied from 2 to 6; however, a steady decrement was observed on a further increase in pH from 6 to 12.

Further, when NaCl salt concentration was varied from 0.001 mol to 0.01 mol, a decrease in viscosity was noticed, which further increases with an increase in salt concentration and undergoes abrupt enhancement at 1 mol NaCl concentration. No impact of pH change (varied from 1–13) was observed at 0.01 mol NaCl concentration, indicating that viscosity becomes independent of pH. This behavior has been associated

with the complete screening of counter-ion effects at 0.01 mol NaCl. So, we can conclude that pH-based rheology of Sul-CNC suspension depends upon only the counter ion effect. However, for carboxylated CNC, both counter ion effect and deprotonation/protonation should be considered because carboxyl groups have higher pKa values than sulphate groups.

Further, CNF, at pH 7, exists in deprotonated form (-ve charged) because of low pKa-4 and forms complex network structures due to their abnormal behaviour(Facchine et al., 2021, 2020; Fukuzumi et al., 2010). Since the microstructure of NC suspension depends on the aspect ratio and morphology of fibrils and due to the higher aspect ratio and flexibility of CNF, these fibrils form complex interactions in suspension, including hydrogen bonding, entanglement and electrostatic repulsion. These complex interactions are responsible for high viscous behavior for pH 7. Pääkkö et al. (Pääkkö et al., 2007) observed an increasing trend in viscosity of low-charged enzymatically pre-treated CNF (≈0.04 meq/g) when the pH of the suspension was decreased from 10.0 to 5.9, 3.8 and 2.0. This behavior has been associated with the screening effect of electrical double layer repulsion from pH 10.0 to 3.8. In contrast, neutralization of the nano fibril charges caused partial coagulation and enhanced viscosity at very low pH: 2, while from pH 10.0 to 3.8. For a highly charged TEMPO-based CNF (≈0.7 meq/g), a decrement in intrinsic viscosity with a decrease in pH was observed (Jowkarderis and van de Ven, 2014). This behaviour has been related to compression of the electrostatic double-layer of charged CNFs; however, at very low pH, coagulation of fibrils occurs and leads to gel formation.

NC suspensions show time-dependent rheological, i.e., thixotropic behavior. Upon shearing or shaking, cellulose suspensions become less viscous, and time is required to recover the lost viscosity. The recovery rates for TO-CNF suspension were noticed to increase with the increase in ultrasonication treatment time (Lee et al., 2020). Also, the time required for 70% recovery of the G′ decreased with increasing ultrasonication time. The higher recovery rate of the TO-CNF suspension developed at 2 min of sonication time than that of suspension created using the high-pressure homogenizer technique has been assigned due to the shortening of the CNFs average length in the later one. Concentration also plays a crucial role in recovery time. It has been noticed that upon enhancing the amount of CNFs, there are more chances for TO-CNFs to come in contact with each other and thus rate of recovery could be improved. The ionotropic characteristic of CNCs suspension depends on concentration and charge density on the CNC surface (Araki et al., 1998). The absence or lack of charge on the surface of Hcl-CNCs results in the aggregation of CNCs, and thus the thixotropic behavior appeared at a much higher concentration, i.e., greater than 0.5% (w/v). However, no thixotropic behavior was noticed for Sul-CNC suspension, even at much higher concentrations. Xu et al. (Xu et al., 2024) during the their study on thixotropic behaviour of both CNCs (amount varied: 4.5, 6.0 and 7.5 wt%) and TO-CNFs (0.3, 0.8 and 1.3 wt%) suspension by employing hysteresis loop tests confirmed that TO-CNFs suspension possess stronger thixotropy and shear stress than CNCs owing to higher aspect ratio and stronger structural network of the former. Furthermore, at low concentrations, 4.5 wt% CNCs suspension exhibited no stress overshoot and hysteresis loop compared to 0.3 wt% TO-CNFs suspension. However, when concentration was raised in both cases, a continual rise in the area under the hysteresis loop was seen, indicating a strong increase in thixotropic behaviour. Kim et al. (Kim et al., 2023) evaluated the impact of addition of TO-CNF (wt% varied from 0.03 to 0.20%) on viscoelastic properties of resulted CNCs suspension. They confirmed increase in viscosities of the resulted suspension with addition of TO-CNF because of the enhanced CNC-CNC interaction due to the screening of the CNC charge due to sodium cation from TO-CNFs (Fig. 11). Further, when TO-CNFs loading was ≤ 0.07 wt% almost all samples exhibited same apparent viscosity, a region called isolation region, however, at higher loading i.e., > 0.07 wt% (region called as contact region) a jump in viscosities was noted. Also, with increase in shear rate a higher shear thinning behavior was observed in contact region than isolation region. The viscosity of CNC suspensions prepared
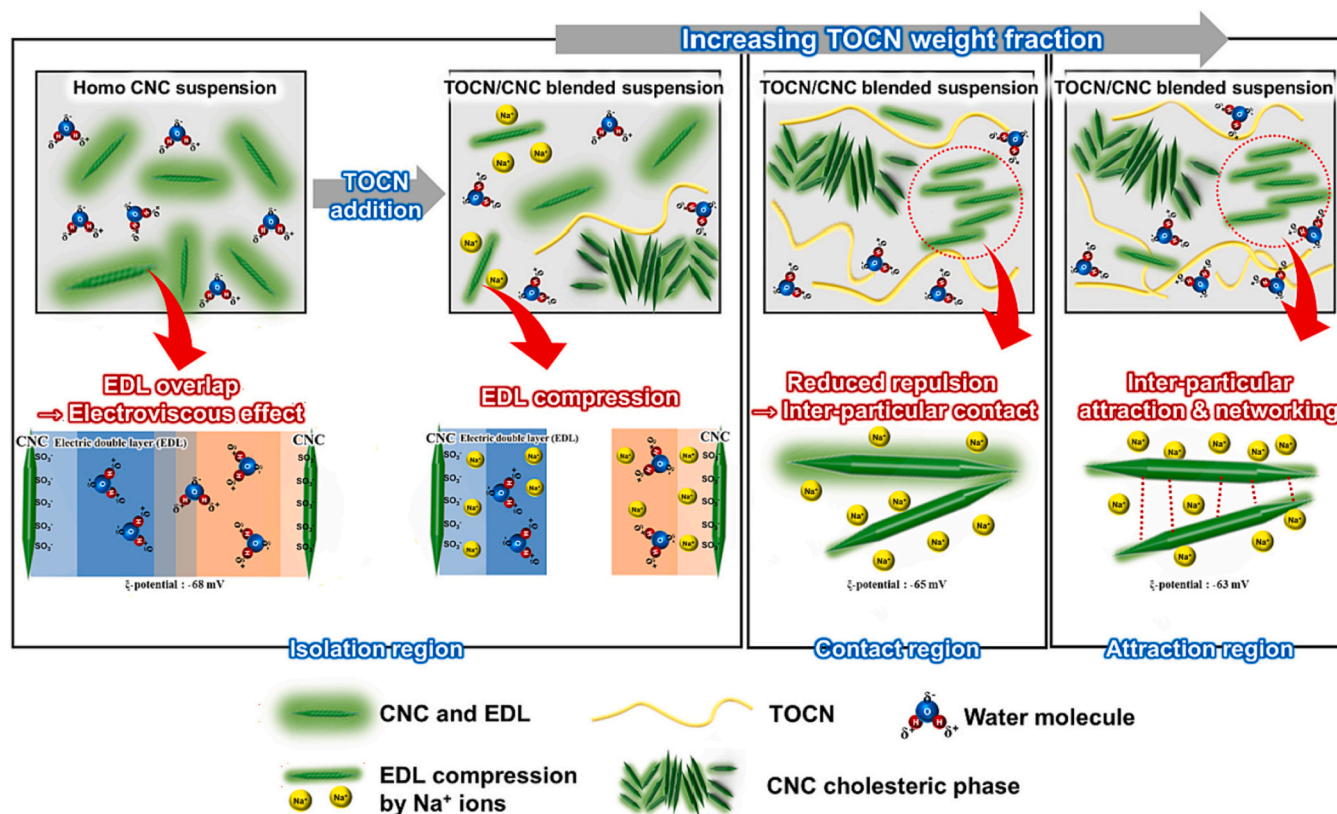
Fig. 11. Schematic view for the change in the electrostatic state and particular interaction of nanocellulose in TOCN/CNC-blended suspensions. [Here EDL and TOCN are electric double layer and TO-CNFs, respectively] (Kim et al., 2023).
"Reprinted with permission from Ref. (Kim et al., 2022) Copyright 2023,Elsevier''.

by using three different techniques, namely ultrasonic treatment, mechanical stirring and high shear homogenization, has been found to increase with time after the settlement of the suspensions (Peng and Via, 2021). Further, mixing the suspension after 60 days, using a magnetic stirrer, a decrement in the viscosity of CNCs suspension up to different levels for various samples, i.e., prepared by using different techniques, was observed. Among different techniques, the ultrasonication and homogenization techniques were found to significantly reduce the viscosity of the suspension over time in comparison to the magnetic stirrer technique.

According to Frka-Petesic et al. (2015), Sugiyama et al. (1992), cellulose has anisotropic diamagnetic susceptibility. In the presence of a powerful magnetic field, the cellulose nanocrystals, as compared to CNFs because of their smaller dimensions, align preferentially with their long axes perpendicular to the field. In order to improve the alignment of CNCs in liquid crystal systems, Zhu et al. (Zhu et al., 2020) used the strength of electric and magnetic fields. To circumvent issues brought on by water's conductivity, the redispersion of CNC in non-polar organic solvents is utmost necessary for their applications in electric fields (Casado et al., 2021; De France et al., 2016). The suspension of low-concentration CNCs can be positioned perpendicular to the applied field to produce a nematic order by exposing it to a strong magnetic field. However, an anisotropic phase appears, in which tactoids become orientated when the concentration of CNCs suspension is raised to a specific higher value. This causes fewer dislocations to exist and a more uniform alignment to be accomplished by orienting the rotating directors of the CNC planes perpendicular to the magnetic field(Revol and Marchessault, 1993). Magnetic fields of suitable strength and CNCs of appropriate aspect ratio and concentration are required to orient CNCs samples. This behavior was confirmed by De France et al. when they applied magnetic fields of 0.56–1.2 T to orient 1.65 and 4.13 wt% CNC suspensions, but found no satisfactory results. Further, both G' and

viscosity of Sul-CNCs suspensions (0.1 and 0.5 wt%) were noticed to be enhanced with an increase in magnetic field from 0–1 T (De France et al., 2016). However, as the concentration of CNCs was further raised, it was shown that the magnetic field less impacted the rheological characteristics of the suspensions due to an increasing steric hindrance effect. Cellulosic materials have also been discovered to exhibit electrorheological responses as a result of water molecules adhering to NC surfaces (Choi et al., 2017).

5.4. Type of additives

Type and concentration of polyelectrolyte or inorganic additives or salt strongly impact the rheology of NCs suspension. Since cellulose binds strongly to water molecules, wet chemistry technologies that lead to cellulose aggregation, flocculation or coating can enhance the percentage of solid contents in the web (Khan et al., 2020). Three different types of polyelectrolytes, namely cationic, anionic and non-ionic polyelectrolytes, have been used to tailor the rheology properties of nano cellulose. Among these, cationic polyelectrolytes, which act as flocculants, have been preferred by several researchers to neutralise the appositively charged cellulosic fibers (Hubbe, 2005; Müller, 2014; Petzold and Schwarz, 2013; Roberts, 2007). Their utility leads to the flocculation of cellulosic nano fibers when the cellulose surface is sufficiently neutralized. Depending upon their charge density and molecular weight, Cationic electrolytes adsorb differently onto cellulose fibers(Aarne et al., 2012; Hubbe et al., 2009; Khan et al., 2020; Roberts, 2007). They penetrate the fibres' pores and diminish the cellulosic fibers' water adsorption tendency. The cationic electrolytes cause strong interactions among the suspensions either through bridging (Raj et al., 2015) or charged patch mechanisms(Lu et al., 2014; Sandell and Luner, 1974). Rarely, an excess of cationic polyelectrolytes may result in the reversal of charge and stabilization of particles in suspensions (Ashmore

et al., 2001). Anionic electrolytes, besides the similarity in negative charge with that of cellulose, showed minor adsorption onto cellulose and impacted the rheology of suspension to a lesser extent (Tardy et al., 2017). Anyway, these polyelectrolytes may also result in larger flocs of fibers compared to cationic electrolytes. In the case of anionic electrolytes, the rheology effects have been attributed to their behavior as a steric stabilizer, as a dispersant, or they may deplete flocculation (Li et al., 2020; Meree et al., 2016; Oguzlu et al., 2016). The last category of polyelectrolytes is nonionic polymer, which usually contains a sufficient number of hydroxyl groups and thus forms a comprehensive hydrogen bonding with the OH groups of cellulose, leading to a remarkable increment in the rheology of nano cellulose suspensions (Li et al., 2020; Meree et al., 2016).

Further, oppositely charged polyelectrolytes are generally mixed to form polyelectrolyte complexes, which subsequently form liquid-phase separated coacervates or solid precipitates(Fu and Schlenoff, 2016; Khan and Brettmann, 2018). Kahn et al. (Khan et al., 2020) studied the interaction between NC and polyelectrolytes coacervates (PEC) of cationic (poly allyl amine hydrochloride; PAH) and anionic electrolytes (polyacrylic acid salt; PAA). The sequential addition of PAA and PAH to CNFs or the addition of preformed coacervates to CNFs has been found to impact the time for the complete association and the strength /extent of PEC association to fibers surface. When preformed coacervates were utilized, loose interaction between fibers and PECs occurred, and complete agglomeration took place in approximately three days. However, upon sequential addition of polyelectrolytes, a significant enhancement in the interaction of the coacervates with the cellulosic fibres was noted. Further, in this case, the complete association was noted to take place within 40 min, leading to faster fibres agglomeration and better water rejection tendency than preformed coacervates addition. Li et al.(Li et al., 2022) reported an increase in the viscosity of sodium alginate (SA) upon the addition of CNFs, while evaluating the rheology of SA/CNF, SA/carboxymethyl chitosan (CCT) and SA/CN/CCT samples; however, upon addition of CCT, an inverse behavior was observed. All three pastes were classified as non-Newtonian fluids, i.e., showing shear thinning characteristics and showed a rapid shear thinning behavior when compared to SA solution. The amount of lignin contents in CNFs strongly influences the rheological properties of suspension of lignin-containing CNFs (LCNFs).

Iglesias et al. (2020) extracted LCNFs from Eucalyptus globulus chips containing different amounts of lignin contents (0.6%, 1.7%, 4.7% and 10.2%) and further evaluated the impact of lignin contents on their rheology. All samples showed an increase in viscosity with an increment in lignin contents and a non-Newtonian shear-thinning behavior with an increase in shear rate. The shear thinning behaviour was confirmed by calculating the power law parameters [Power law: $\tau = k\gamma^n$, here τ, k, γ and n represent shear stress (Pa), consistency coefficient, i.e. reveals the relationship between shear rate and shear stress (Pa s^{-1}), shear rate (s^{-1}) and flow behavior index, respectively], in which the values of n were found to be < 1 for all samples. Further, the value of G' was found to be higher than G'' for all samples along the entire frequency range, confirming gel-like characteristics for these samples. Also, with an increase in lignin contents, enhancements in values of G'' and G' were reported. The pure anionic polyelectrolyte, CCT, when combined with different BC (0.01 - 0.2 wt%) suspensions, displayed shear thinning behavior (Zhang et al., 2022). The various suspensions showed a high and gradual decrease in viscosity at pH 7 than pH 9.2 because of the entanglement of BC and carboxymethyl cellulose (CMC) at lower pH. Further, all samples displayed gel-like characteristics (here G' value dominates over G''), and moduli were noted to be dependent slightly on the frequency. Shear thinning behavior was observed for composite hydrogels of CNFs and gum Arabic (Wu et al., 2022). However, the initial viscosity and extent of viscosity of different suspensions of CNFs and gum Arabic (CNF+Gum Arabic; 0.3 gm & 0.15 gm; and 0.3 & 0.3 gm, respectively) and their suspension (CNF+Gum Arabic; 0.3 gm each) sonicated for 30 min at 400 and 600 w, found to depend on the sonication power and their

composition strongly. The decrement in viscosity with an increase in shear rate has been attributed to the elongation and disintegration of the hydrogels.

The interaction of CNCs with two different anionic electrolytes, namely CMC and SA, was studied using steady and dynamic rheological instruments with or without CaCl$_2$ cross-linker (Cui et al., 2022). Improvements in rheological characteristics of SA and CMC were noted after the addition of varying amounts of CNCs (1–7 wt% CNCs). During the calculation of flow curve gradients utilizing the power law model $\tau = k\gamma^n$, variation from Newtonian flow behavior was confirmed (Wang et al., 2022a,2022b). In general, the greater the variation of 'n' value for a suspension from 1, the more will be its non-Newtonian flow behavior. For both solutions, i.e., CMC-CNCs and SA /CNCs, the n values were found to be less than one, thus indicating pseudoplastic fluids characteristic of the solutions (Feng et al., 2021). Further, among CMC-CNCs and SA /CNCs samples, greater deviation (decreasing trend; 0.8 to 0.2 approx) in 'n' values from 1 and an increase in k values (from 0.1 to 5 Pa S^n) with an increase in the concentration of CNCs was observed in case of the former one, indicating higher shear thinning behavior of CMCs solution after addition of CNCs; however, in case of SA /CNCs, non-significant variation in 'n' value (approx. 0.64 for all samples) and a decreasing trend in k value (approx. 17 to 15.5 Pa S^n) was observed. Further k value for SA/CNCs was noticed to be higher than CMC/CNC indicating the need of greater shear stress to produce same shear rate (Vickers et al., 2015). Further, the elastic modulus and viscosities of CMC were positively co-related to CNCs amounts in alkali, neutral or acidic conditions. When the contents of CNCs content was > 5% at pH 9.45, the acceleration in gelation of CMC was noticed. For all suspensions, the tan δ value decreased with an increase in the angular frequency values, representing more viscous characteristics for both CMC/CNCs and SA/CNCs at the lower frequency region and higher elastic characteristics at the longer frequency region. Further, between CMC/CNC and SA/CNCs samples, the G' values of the former system, was noticed to be significantly enhanced, while the tan δ values decreased when the CNCs concentrations was varied from 1–7 wt% at low angular frequency. But at higher angular frequencies, the elastic modulus and damping factor converged to the CMC's flow curve. However, no significant differences in G'and tan δ of the SA composite samples were observed after the addition of CNCs. Further, an increase in tan δ and a decrement in the G' of CMC was noted when calcium salt concentration was increased. Such behavior has been attributed to characteristics of anionic CMC polyelectrolytes. However, an opposite trend was found in the case of the SA/CNCs system, and when calcium ions amounts were> 0.07%, the tan δ of the SA system was noticed to be < 1, which clearly indicates gel transformation of the SA system. A ternary mixture of gelatin, cationic CNCs and hyaluronic acid (HA) showed an increase in viscosity with an increase in the concentration of CNCs from 2 to 5 wt% (Warwar Damouny et al., 2022). However, a sharp decrease in viscosity was observed for 5 wt% CNCs loaded samples at a higher pressure, and their viscosity was found to be lesser than even that of 2 and 3 wt% CNC concentrated samples. Chitosan and xyloglucan have recently been employed by Leray et al. (2022) to regulate the rheology of CNCs. They first combined a specific amount of CNCs and xyloglucan to create the various suspensions [R 0.2, R 0.5, and R 1; which contained nanocrystals 1% w/w and xyloglucan at a concentration 0.2% w/w, 0.8% & 0.4% w/w, and 0.6% each w/w, respectively. They then coated the suspensions with a 0.1% w/w solution of chitosan to create a film. For synthetic films (R0.2, R0.5, and R1), G' was discovered to be higher than G'', confirming the gel-like behaviour of the films. Upon increase in xyloglucan/CNC concentration, both G' and G'' was noted to decrease, reflecting an enhancement in the rigidity of suspension after addition of CNCs.

Including inorganic nanoparticles (NPs) may effectively enhance the rheological properties of nano cellulose solutions. Liu et al. (Yuan et al., 2021) studied the interaction of three NPs, namely AlOOH, SiO$_2$, and ZnO, having different sizes and charges, with carboxylic-CNFs (CCNFs)

suspension. They concluded that at low shear rates (<0.1 s^{-1}), all NPs loaded samples, i.e., 0.4 wt% CNF+ (0.0, 0.1, 0.2, 0.3 & 0.5) wt% AlOOH, 0.4 wt% CNF+ (0.1, 0.2, 0.3& 0.5) wt% SiO$_2$ and 0.4 wt% CNF+ (0.0, 0.1, 0.2, 0.3& 0.5) wt% ZnO systems showed the characteristics of Newtonian fluid. However, at the shear rate $0.1 - 1000$ s^{-1}, all samples showed shear thinning behaviour, i.e., non-Newtonian characteristics.

The samples' viscosity was found to vary with the types of NPs added. For example, (Fig. 12 a-f) on the addition of AlOOH NPs, the viscosity of the CCNF system was enhanced, while for SiO$_2$ and ZnO NPs loaded systems, a decrement in viscosity was noted. Further, through the dynamic rheology responses, it has been affirmed that for the CCNF sample, G$'$ > G$''$ in the relatively low-frequency region (0.01 to 1.75 Hz), showing typical elastic behavior (Fig. 12 a-f). However, above 1.75 Hz, G$'$ < G$''$ was noted, indicating the viscous behaviour of the CCNF system. The inclusion of AlOOH NPs in the CCNFs system results in the enhancement of both G$'$ and G$''$. However, a region where G$'$ > G$''$ expands continuously with an increase in wt% loading of AlOOH NPs indicating elastic behavior for CCNF+ AlOOH systems more evidently. In contrast, in the case of CCNF/ZnO and CCNF/SiO$_2$ systems, G$'$ < G$''$ was noticed. An increase in the difference of values of G$'$ and G$''$ was found with further increase in NPs contents, indicating more prominent viscosity in CCNF/ZnO and CCNF/SiO$_2$ systems. Whereas, in the case of the CCNF/AlOOH system, with an increase in NPs concentration, enhancement in viscoelasticity was noticed. Different forces such as hydrogen bonding, electrostatic interaction, ion binding and hydrophobic interaction in between polymers and NPs generally impact the rheological properties of systems(Hu et al., 2017; Xu et al., 2021). However, in the present case, both CCNF and NPs are hydrophilic by nature, thus, hydrogen bonding and hydrophobic forces have been ignored. It was concluded that only the size and electrical characteristics of CCNFs and NPs impact or control the interaction and, ultimately, the rheological characteristics of systems.

Salt ionic strength greatly influences the charge-induced electric double layers on nano cellulose surfaces (Bertsch et al., 2017). However, van der *Waals* forces that momentarily result from fluctuating dipoles remain unaffected by ionic strength (Adair et al., 2001). The compression of the electric double layer after the addition of salts upsets the equilibrium between electrical double layer repulsion and van der *Waals* attraction, directly affecting the rheological characteristics and colloidal stability of charged NC suspensions (Boluk et al., 2011; Shafiei-Sabet et al., 2014). Researchers have studied the suspensions of NC and their nematic phase transition behavior utilizing rheometry (Oguzlu et al., 2017; Shafiei-Sabet et al., 2016). High salt concentrations have been discovered to cause agglomeration of CNCs, which eventually form hydrogels. Various agglomeration processes have been postulated based on the use of divalent and monovalent salts (Chau et al., 2015; Lenfant et al., 2017). Intermolecular ionic bridges have been suggested for the divalent ion Ca^{2+}. It has also been predicted that after the addition of salt, CNCs will aggregate due to the dominance of attractive forces following a decrease in electrostatic repulsion. Depletion, Van der *Waals*, and hydrophobic interaction have also been predicted to occur in CNCs suspensions (Dong and Gray, 1997; Tang et al., 1996).

Bertsch et al. (Bertsch et al., 2017) investigated the effects of mono- (Na$^+$ and K$^+$) and divalent (Mg^{2+} and Ca^{2+}) metal chloride salts on Sul-CNCs suspension gelation and nematic ordering ability. They found a significant relationship between G$'$ and the zeta-potential value of CNCs' suspension. A strong decrease in zeta potential value and hydrogel formation was seen for divalent cation at low salt concentrations because of effective charge screening. However, in the case of mono-cation salt, the same zeta-potentials and gel strengths were reached at comparatively higher concentrations. They came to the conclusion that the charge screening effect, rather than cation valency, governs intermolecular interactions in CNCs aggregation. As a result, the zeta potential of CNCs hydrogel can be used to control its characteristics. During the evaluation of G$'$, for CNCs suspension consisting of different salts, it was discovered that adding a small quantity of metal chloride salts decreases the elastic properties of suspension. This is because the effective radius of suspension decreases when an electric double layer is compressed, a phenomenon known as the electroviscous effect (Shafiei-Sabet et al., 2014). As the salt concentration was raised further, it was discovered that G$'$ had improved, displaying increased interaction (shown as a dotted box in Fig. 12 g-j) without agglomeration of CNCs because of less electrostatic repulsion. A further increase in salt content causes CNCs to clump together, forming hydrogel with a constant G$'$ value. In another study, on varying valency, i.e. counterions from monovalent (Li$^+$, Na$^+$, and K$^+$) to divalent (Ca^{2+}& Mg^{2+}) and to trivalent (Al^{3+}), a considerable impact on network formation tendency in CNCs suspension has been observed (Nyamayaro et al., 2023). CNC suspensions with various monovalent counterions were found to be anisotropic, bi-isotropic with chiral nematic structures, and form birefringent gels at 3, 5 and 7 wt% concentration, respectively. Monovalent ion-containing CNCs suspensions displayed comparable steady shear viscosity and linear viscoelastic characteristics. The di- and trivalent counterions at all concentrations encourage network development or gel-like properties in contrast to monovalent ions. Additionally, sonication of CNC samples with monovalent ions resulted in a two-folds-of-magnitude reduction in viscosity; however, with multivalent counterions, the reverse trend was seen due to the creation of a strong network. Additionally, it has been observed that the G$'$ rises over time with an increase in radius (i.e., Sn^{2+}>Ca^{2+}>Mg^{2+}) as well as valency of metal cations (i.e., Al^{3+}>Mg^{2+}> Na$^+$) (Dinand et al., 1999; Lenfant et al., 2017). Interestingly, the cation's valence had a greater impact on the rheology of Sul-CNC suspensions than the radius of the cation, confirming that the inter - crystal's bridging ability of multivalent cations is the primary cause of the gelation of Sul-CNC suspension.

In fact, due to the lack of any charge, untreated CNFs should be highly tolerant to ionic strength. However, a minuscule amount of hemicelluloses and pectin-like impurities still remained in CNFs after their extraction from cellulosic wastes and further purification, which further contributed to the presence of certain acids more specifically uronic acid on the CNFs surface (Agoda-Tandjawa et al., 2010; Dinand et al., 1999). Since uronic acid is –ve charged and thus played a vital role in the salt-dependent rheology of untreated CNF solution (Lowys et al., 2001; Sim et al., 2015). The screening effect of electrostatic repulsion between -ve charged CNFs causes an increase in the values of viscosity and G$'$ for untreated CNFs with an increase in salt concentration up to a certain threshold point, leading to fibre's aggregation. However, beyond the threshold value, a decrement in CNF's viscosity has been noticed (Lowys et al., 2001). A decrease in viscosity, when fibres contain polarizable groups like carboxymethylated or carboxylated groups, with a rise in ionic strength, has occasionally also been observed (Jowkarderis and van de Ven, 2014; Naderi et al., 2014a; Tanaka et al., 2014). Since these groups possess a higher surface potential (carboxylate:75 mV; carboxymethyl: 590 leq/g) than hydroxyl groups (25 mV), this leads to a comparatively higher shear viscosity, electrostatic repulsion between CNFs and a distinct type of fibre-fibre interaction (Naderi et al., 2014a). Screening these forces causes the current fibre network to collapse, which lowers the gel's shear strength qualities.

The cation valency similarly influences the rheological characteristics of TO-CNF suspension, just like those of CNCs. According to the report, adding salts with different valencies (AlCl$_3$, MgCl$_2$, and NaCl) at a concentration of 40 mmol/L can each cause gelation of the TO-CNF suspension to a different extent; that is, the CNF suspension becomes increasingly non-uniform as the valency increases(Geng et al., 2017). The gelation of CNF suspension by cations has been linked to decreased Debye length and the increased electrostatic repulsion between the CNFs. The interfibrillar hydrogen bonding and Van der *Waals* forces merge to create two main forces that maintain the CNF linkage. Furthermore, different cation quantities were used to remove the effect of debye length from the equation.

Nevertheless, it was observed that the viscosity of CNFs improved
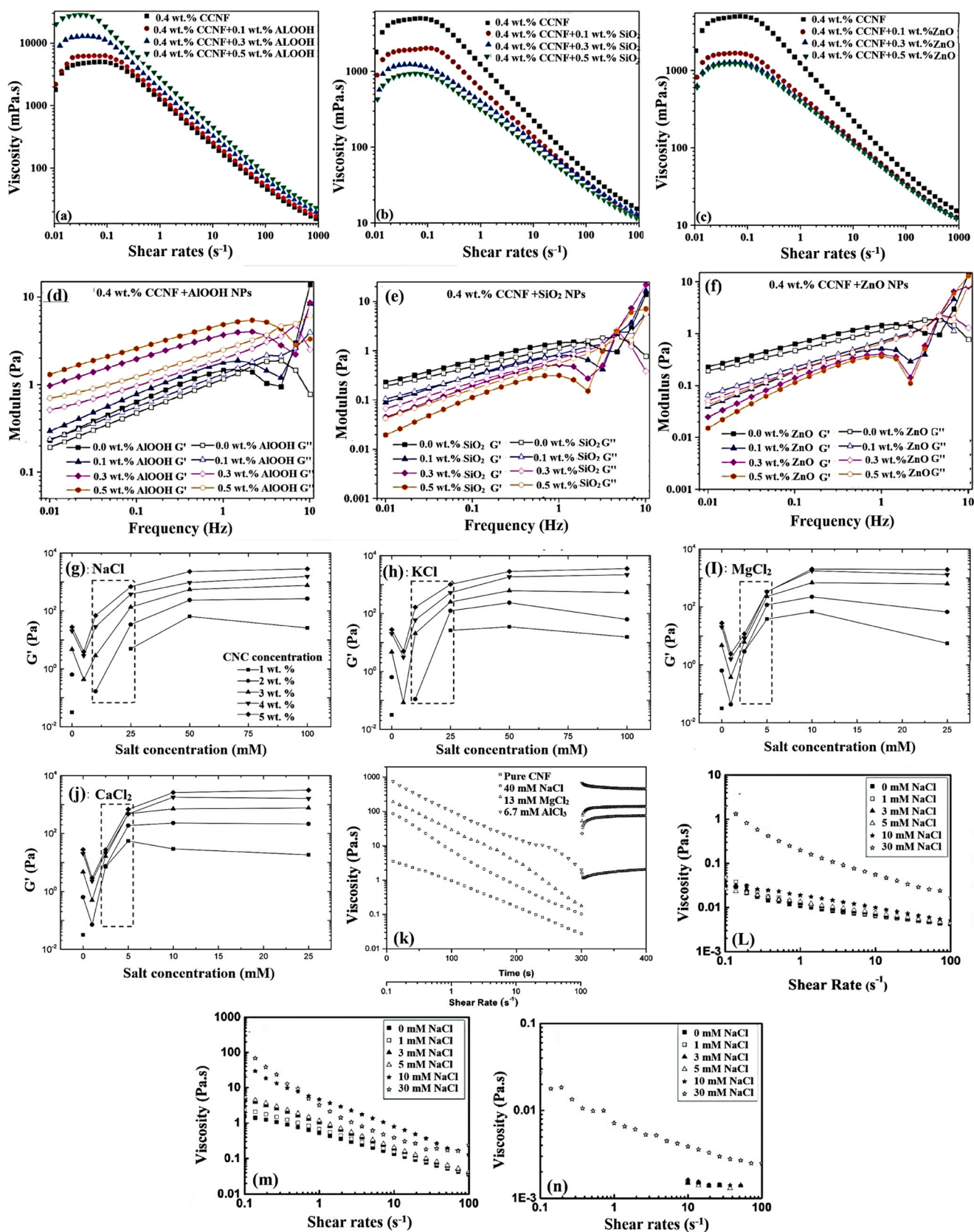
Fig. 12. Steady rheology (a, b and c) and dynamic rheology (d, e and f) of CCNF/NPs (Yuan et al., 2021). Copyright {2021} ACS.", G′ for different CNCs suspension concentrations consisting of (g) NaCl, (h) KCl, (i) MgCl₂, and (j) CaCl₂. The dotted box shows the transition regime where nematic ordering was discovered (Bertsch et al., 2017). Copyright {2017} ACS].

(a) [Fig a-f"Reprinted with permission from reference (Yuan et al., 2021). (b) [Fig g-j "Reprinted with permission from reference (Bertsch et al., 2017). (c) Copyright {2017} ACS."] and Effect of the NaCl concentrations on rheology of CNF suspensions having different concentrations (k) 0.05 wt%, (l) 0.2 wt% and (m) 0.6 wt%; (n) shear viscosity of 0.6 wt% CNF gel with various ions as a function of shear rate and their recovery behavior [Fig k-n "Reprinted with permission from reference (Geng et al., 2017).

as the valency of the cations increased, demonstrating the significance of cation valency as a strong cross-linking agent (Fig. 12 k). Further analysis of the effects of relative CNF concentrations (0.05, 0.2, and 0.6 wt%) and NaCl salt concentrations (1, 3, 5, 10 and 30 mmol/l) on the rheological characteristics of CNF suspension revealed that at very low CNF concentrations (0.05 wt%), the viscosity begins to increase at 30 mmol/L salt concentration; however, at intermediate (0.2%) and relatively higher (0.6 wt%) CNF suspension, the critical salt values drop to about 10 and 3 mmol/L, respectively (Fig. 12 l-n). In other words, the critical NaCl concentration falls as CNF concentration rises, and this is due to both an increase in the number of nanofibers at higher CNF concentrations as well as enhancement in the amount of counterions, which reduce the electrostatic repulsion forces between the CNFs. Reduction in the electrical double layer with an increase in salt concentration has been reported for TO-CNFs by Mendoza et al. (Mendoza et al., 2018) and is supposed to cause an imbalance in repulsive and attractive forces required for a stable colloid. The thickness of the double layer was estimated as a function of ionic strength using the Gouy-Chapman equation. Further, the addition of salt resulted in the release of water from the fibers surface and charge shielding because of the depletion of electrical double layers between CNFs.

5.5. Postprocessing techniques

Due to the higher association capability of NC, these materials are mostly generated as aqueous dissolutions at low solids content, leading to irrational ecological effects and high costs during their transport for large-scale applications in industries, thus remarkably inhibiting their broader utilization (Nordenström et al., 2021). To achieve large-scale NC creation, completely dried materials or suspensions with higher solids content are required (Naderi et al., 2015a). However, when NC is dried, its nanoscale dimensions are lost due to excessive association caused mainly by hydrogen bonding, hornification and attractive van der *Waals* forces (Fernandes Diniz et al., 2004; Li et al., 2021). Hence, aggregation should be avoided to enhance their redispersibility, as it will not enable the original suspension to recover its parent rheological characteristics. Several possible methods have been described in the literature to avoid this aggregation, which include the introduction of a sterically stabilising component by covalent grafting(Kaldéus et al., 2018), enhancement of surface charge density(T, 1982), or utilization of redispersing agents (Laivins and Scallan, 1993; Nordenström et al., 2021). Enhancing the surface charge density is quite impressive. Still, in this technique, one has to compromise with the particle size, molecular mass and dewatering characteristics of cellulose on account of its charge. The graft copolymerization technique is also restricted and not preferred since it is very difficult to carry out grafting on a large scale, and it also irreversibly alters the characteristics of the CNFs. To enhance the redispersibility, utilizing redispersing agents has been preferred because of its negligible impact on the overall properties of NC. Various types of redispersing agents utilized for NC are polyethylene glycol (PEG) (Cheng et al., 2015; Nordenström et al., 2021; Reid et al., 2017), lignin (Nordenström et al., 2021), glycerol (Moser et al., 2018), CMC (Butchosa and Zhou, 2014; Herrick, 1984; Naderi et al., 2015a; Nordenström et al., 2021)and saccharides (Abdelwahed et al., 2006). Several methods to utilize redispersing agents have been discussed in the literature (Butchosa and Zhou, 2014; Cheng et al., 2015; Herrick, 1984; Moser et al., 2018; Naderi et al., 2015a; Reid et al., 2017). Generally, to achieve the desired redispersion, the amounts of redispersing agents were kept at 30 to 50 wt% higher than CNFs (Missoum et al., 2012; Moser et al., 2018; Naderi et al., 2015a). However, desirable results were also found in some cases even with a small quantity of redispersing agents (Moser et al., 2018; Naderi et al., 2015a). Nordenström et al. (Nordenström et al., 2021) enhanced the redispersibility of freeze-dried TO-CNFs by adding three different redispersing agents, namely PEG, CMC or lignin. Out of which, lignin, even at a very low 5 wt%

concentration with respect to CNFs, was found to provide better redispersion characteristics compared to other redispersing agents. This behaviour has been attributed to better steric repulsion, i.e., low agglomeration of CNFs. The redispersing tendency of CNF nanopapers and freeze-dried CNF dispersions was compared, and it was demonstrated that the former, even without including redispersing agents, led to better redispersion of CNFs. Further, in the case of the nanopaper technique, preservation of mechanical toughness and a non-significant change in the size of CNFs were noted after redispersion. Such behavior has been attributed to the generation of a suitable structure during filtration, causing better dispersion of CNF's. However, in the case of the freeze-drying process, inevitable ice crystal generation was found to cause agglomeration of CNFs. Further, nanopapers designed from the redispersed CNFs showed the same mechanical toughness as those prepared from never-dried CNFs. Hence, all the above discussion suggests that converting CNFs suspensions into nano paper is eco-friendly and economical and could be viable for their large-scale application without compromising their mechanical toughness. Redispersing capability of sugar beet-based CNFs has been preserved by partial removal of hemicelluloses and pectin contents from CNFs, and it has been noted that CNFs containing a higher amount of hemicelluloses and pectin contents retain approximately 80% of the rheological characteristics of the original CNFs suspension (Hietala et al., 2017). Here, hemicelluloses and pectin minimize the hydrogen bond formation tendencies between CNFs because of physical blocking and electrostatic repulsion, promoting CNFs redispersion. Kim and colleagues (Kim et al., 2022) discovered that adding lignin to the suspension of CNFs reduced the likelihood for fibres to clump together throughout the drying and dehydration processes and also guaranteed outstanding redispersion kinetics and integrity. Additionally, the unwanted lignin might be eliminated with an easy washing process. It was proven that the inclusion of lignin made it possible for the dehydration, redispersion, and polymer processing techniques to revert the CNFs chemical and physical properties comparable to that of pristine or never-dried CNFs. The potential of sodium chloride salt to regulate the hydrogen bonding between CNFs and prevent them from adhering together during the drying process was also investigated and it was shown that this method may also improve the CNFs' redispersibility (Ma et al., 2021). It has also been established that dried CNFs, produced by using lime residue, may be easily redispersed while preserving their original physico-chemical properties(Jongaroontaprangsee et al., 2018). Pectin, which is naturally present in citrus leftovers, has been linked to this characteristic, which prevents the hornification of CNFs during drying process.

6. Current barriers and their potential solutions

The synthesis of nanocellulose is still confronting various barriers, such as chemical recovery problems, high energy consumption, and complicated and costly purification methods, which have restricted its large-scale deployment. The higher energy consumption can be reduced by employing suction and pressing techniques instead of heat to dry nanocellulose. Solvent recovery can be enhanced by utilisation of carbon adsorption process or solvent scrubbing technique.

Further, to avoid the usage of hazardous chemicals, which require complex and advanced post-processing techniques, the green approaches such as ball milling, enzymatic hydrolysis, deep eutectic solvents, etc., can be employed for bulk extraction of nanocellulose from raw plant wastes. Out of various techniques deep eutectic solvent technique gives quite promising results and is economical than ball milling and enzymatic hydrolysis techniques. However, still more efforts are needed to optimize deep eutectic solvent-based extraction process, especially the reusing and recycling process, in order to significantly reduce the economic costs of nanocellulose. Despite the fact the nanocellulose is green, non-toxic and environment friendly but still further studies are required to investigate the impact of nanocellulose on human health.

Another key impediment to the inclusion of nanocellulose in the oilfield is the inability of work procedures to be repeated, despite the fact that the literature is rich with numerous strategies which can be employed for extraction or synthesis of CNFs and CNCs from diverse non-traditional sources.

Furthermore, under severe conditions (high pressure, high temperature, and high salinity), nanocellulose-based fluids might show irregular flow, undergo thermal deterioration, and saline-induced aggregation. These issues can be solved by using adequate surface modification techniques or by adding relevant additives, which will bestow nanocellulose with desired properties such as high salt tolerance, amphiphilicity, etc., and thus can be solely utilized as nano oil displacing agent either alone or along with non-ionic surfactant to enhance the oil recovery. Likewise, the use of solvents during surface functionalization should be limited to avoid poor redispersion of hydrophobically functionalized nanocellulose in water.

Oil recovery can be enhanced by optimization of nanocellulose amount, temperature, additives, etc. Further, the use of nanocellulose in fluid for enhanced oil recovery may result in an enormous amount of waste, thus efforts are needed to recycle or effectively treat the nanocellulose from the fluid wastes, which may further boost the oil industry's economical, viable, and carbon-free growth. The majority of investigations on nanocellulose-based fluids for increased oil recovery were conducted on a laboratory scale, and were carried out by studying the rheology of nanocellulose based fluids in artificial conditions. Thus, a practical oilfield investigation is critical to determine whether the nanocellulose is applicable in oil industry and the experimental findings from laboratory conditions are reliable.

7. Conclusion, future prospectives and current challenges

A comprehensive knowledge of the rheology of NCs in aqueous media is essential for its potential use in the oil field sector. Rheology of NCs in aqueous suspensions plays a vital role in achieving effective pumping and mixing of this material during production. NCs in an aqueous medium form interconnected networks exhibiting gel-like, shear thinning and thixotropic behavior. The strength of these networks increases with enhancement in cellulose concentration and ionic strength. At different temperatures, the CNC suspensions at low concentrations showed a continuous decline in viscosity with an increase in shear rate and viscosity was noticed to decrease with an increase in temperature, while upon further increase in concentration, suspension becomes predominately anisotropic, showing three region behavior and viscosity increases after a certain temperature; however, on further increase in concentration, all samples showed a continuous decline in viscosity with shear rate and viscosity was noticed to increased significantly at a higher temperature.

The temperature showed little or no impact on the strength of CNF in the linear viscoelastic region; however, their viscosity increased during flow measurements. Further, when NCs suspension was prepared with chemically free techniques, a higher tendency of NC suspension to flocculate was noticed; however, for chemically treated NCs, the suspension was noticed to be comparatively stable. This behaviour has been associated with the development of negative/positive charge onto fiber/particle surface, leading to better repulsion between fibers and thus, better colloidal stability. Keeping in view the agglomeration tendency of chemically free synthesised NCs, more specifically CNFs, their interpretation utilizing plateplate or cone-plate geometries should be avoided, because here, the size of formed flocs may match the geometry gap. Thus suspensions may be prone to wall depletion and phase separation. Thus, in case other geometry like wide-gap couette with roughened surfaces might be a good option. The chemically treated CNF suspensions may be accepted to be less impacted by the rheometer geometry gap, but still wall depletion effect cannot be ignored here. Anionic and nonionic polyelectrolytes, as steric stabilizers/dispersants, displayed a strong tendency to deplete the flocculation of CNFs as well as to stabilize

the CNCs suspension. In addition to polyelectrolyte (anionic and nonionic polyelectrolyte), inorganic nanoparticles (AlOOH, SiO_2, and ZnO) and inorganic salts, NCs aqueous suspension demonstrated non-Newtonian shear-thinning behavior with an increase in shear rate. The NCs suspension at a low percent addition of inorganic particles addition displayed Newtonian flow behaviour at a low shear rate, while at a higher shear rate non-Newtonian shear thinning behavior was observed. pH of suspension also plays a key role in defining the overall rheology of NCs suspension. When varied below or above the pKa value, it causes deprotonation or protonation of functional groups available onto NCs surface and thus may lead to stronger or weaker NCs network. Any material having a zeta potential value higher than $\geq \pm 30$ will be colloidally stable. But, when zeta potential values are lower than absolute value 30, particles may agglomerate and thus affect the rheology of NCs.

NCs suspension showed thixotropic behaviour; however, concentration, charge density and size are the factors which must be taken into consideration while studying NC's thixotropic behaviour. For transporting purposes, various post-processing techniques have been developed to reduce the chances of loss of nanoscale dimensions of NCs because of agglomeration. In this context, various redispersing agents like polyethylene glycol, lignin, glycerol, CMC and saccharides were tested. Efforts are still required in this field on a large scale to retain the rheological characteristics of NCs. It is of utmost importance to develop highly efficient and reliable technologies for rheological characterization of NC suspensions, considering NCs types, geometry, surface charges/roughness, etc. Endeavors should be made in developing new and advanced techniques to tune the rheological characteristics of NC suspensions more rapidly and efficiently for the desired purposes.

From the above discussion, it can be inferred that NCs have huge potential to be employed in the oil industry. However, there are still certain challenges which must be taken into consideration. In comparison to custom-made synthetic additives, NCs lack specified surface chemistry and structural uniformity. Even though industrial-level manufacturing of NCs is now a reality, however its cost is still quite high when compared to synthetic additives and surface functionalization will increase its cost even further. Furthermore, technical developments are likely to lower the cost of nanocellulose manufacturing, enabling large-scale applications in the oil field sector feasible in the future. Pilot plant and field trials are necessary to determine the behaviour of NCs in oilfields.

Engineers should have thorough knowledge of NCs selection criteria and their performance under different reservoir conditions. For effective utilization of NCs in electrocoalescence, a technique mostly employed to dehydrate emulsions, the behaviour of NCs at the interface of oil-water emulsions should be thoroughly studied under varied electric fields. Finally, researchers should strive to integrate NCs with other advanced additives, most likely inorganic nanoparticles, to improve oil recovery even further.

Declaration of Competing Interest

The authors declare that they have no known competing financial interests or personal relationships that could have appeared to influence the work reported in this paper.

References

Aadland, R.C., Jakobsen, T.D., Heggset, E.B., Long-Sanouiller, H., Simon, S., Paso, K.G., Syverud, K., Torsæter, O., 2019. High-temperature core flood investigation of nanocellulose as a green additive for enhanced oil recovery. Nanomaterials 9, 665.

Aarne, N., Kontturi, E., Laine, J., 2012. Influence of adsorbed polyelectrolytes on pore size distribution of a water-swollen biomaterial. Soft Matter 8, 4740. https://doi.org/10.1039/c2sm07268h.

Abdelwahed, W., Degobert, G., Stainmesse, S., Fessi, H., 2006. Freeze-drying of nanoparticles: formulation, process and storage considerations☆. Adv. Drug Deliv. Rev. 58, 1688–1713. https://doi.org/10.1016/j.addr.2006.09.017.

Adair, J.H., Suvaci, E., Sindel, J., 2001. Surface and Colloid Chemistry. In Encyclopedia of Materials: Science and Technology; Buschow, K.H.J., Cahn, R.W., Flemings, M.C., Ilschner, B., Kramer, E.J., Mahajan, S., Veyssière, P., Eds.

Agoda-Tandjawa, G., Durand, S., Berot, S., Blassel, C., Gaillard, C., Garnier, C., Doublier, J.-L., 2010. Rheological characterization of microfibrillated cellulose suspensions after freezing. Carbohydr. Polym. 80, 677–686. https://doi.org/10.1016/j.carbpol.2009.11.045.

Araki, J., Wada, M., Kuga, S., Okano, T., 1998. Flow properties of microcrystalline cellulose suspension prepared by acid treatment of native cellulose. Colloids Surf. Physicochem. Eng. Asp. 142, 75–82. https://doi.org/10.1016/S0927-7757(98)00404-X.

Armstrong, C.D., Yue, L., Deng, Y., Qi, H.J., 2022. Enabling direct ink write edible 3D printing of food purees with cellulose nanocrystals. J. Food Eng. 330, 111086 https://doi.org/10.1016/j.jfoodeng.2022.111086.

Ashmore, M., Hearn, J., Karpowicz, F., 2001. Flocculation of latex particles of varying surface charge densities by chitosans. Langmuir 17, 1069–1073.

Ates, B., Koytepe, S., Ulu, A., Gurses, C., Thakur, V.K., 2020. Chemistry, structures, and advanced applications of nanocomposites from biorenewable resources. Chem. Rev. 120, 9304–9362. https://doi.org/10.1021/acs.chemrev.9b00553.

Barnes, H.A., 1995. A review of the slip (wall depletion) of polymer solutions, emulsions and particle suspensions in viscometers: its cause, character, and cure. J. Non-Newton. Fluid Mech. 56, 221–251. https://doi.org/10.1016/0377-0257(94)01282-M.

Beluns, S., Gaidukovs, S., Platnieks, O., Gaidukova, G., Mierina, I., Grase, L., Starkova, O., Brazdausks, P., Thakur, V.K., 2021. From wood and hemp biomass wastes to sustainable nanocellulose foams. Ind. Crops Prod. 170, 113780 https://doi.org/10.1016/j.indcrop.2021.113780.

Bertsch, P., Isabettini, S., Fischer, P., 2017. Ion-Induced hydrogel formation and nematic ordering of nanocrystalline cellulose suspensions. Biomacromolecules 18, 4060–4066. https://doi.org/10.1021/acs.biomac.7b01119.

Beugre, E.Y.-M., Gnagne, T., 2022. Vane geometry for measurement of influent rheological behaviour in dry anaerobic digestion. Renew. Sustain. Energy Rev. 155, 111928.

Beyene, D., Chae, M., Dai, J., Danumah, C., Tosto, F., Demesa, A., Bressler, D., 2018. Characterization of Cellulase-Treated Fibers and Resulting Cellulose Nanocrystals Generated through Acid Hydrolysis. Materials 11, 1272. https://doi.org/10.3390/ma11081272.

Biliuta, G., Dascalu, A., Stoica, I., Baron, R.I., Bejan, D., Bercea, M., Coseri, S., 2023a. Structural and rheological insights of oxidized cellulose nanofibers in aqueous suspensions. Wood Sci. Technol. 1–23.

Biliuta, G., Dascalu, A., Stoica, I., Baron, R.I., Bejan, D., Bercea, M., Coseri, S., 2023b. Structural and rheological insights of oxidized cellulose nanofibers in aqueous suspensions. Wood Sci. Technol. 57, 1443–1465. https://doi.org/10.1007/s00226-023-01505-2.

Bist, N., Nair, A., Yadav, K., Sircar, A., 2023. Diverting agents in the oil and gas industry: a comprehensive analysis of their origins, types, and applications. Pet. Res., S2096249523000698 https://doi.org/10.1016/j.ptlrs.2023.09.004.

Boluk, Y., Danumah, C., 2014. Analysis of cellulose nanocrystal rod lengths by dynamic light scattering and electron microscopy. J. Nanopart. Res. 16 (1), 7.

Boluk, Y., Lahiji, R., Zhao, L., McDermott, M.T., 2011. Suspension viscosities and shape parameter of cellulose nanocrystals (CNC). Colloids Surf. Physicochem. Eng. Asp. 377, 297–303. https://doi.org/10.1016/j.colsurfa.2011.01.003.

Butchosa, N., Zhou, Q., 2014. Water redispersible cellulose nanofibrils adsorbed with carboxymethyl cellulose. Cellulose 21, 4349–4358. https://doi.org/10.1007/s10570-014-0452-7.

Cainglet, H.E., Tanner, J., Nasiri, N., Browne, C., Garnier, G., Batchelor, W., 2023. Rapid cellulose nanomaterial characterisation by rheology. Cellulose 30, 4971–4982. https://doi.org/10.1007/s10570-023-05180-1.

Carneiro Pessan, C., Silva Bernardes, J., Bettini, S.H.P., Leite, E.R., 2023. Oxidized cellulose nanofibers from sugarcane bagasse obtained by microfluidization: Morphology and rheological behavior. Carbohydr. Polym. 304, 120505 https://doi.org/10.1016/j.carbpol.2022.120505.

Casado, U., Mucci, V.L., Aranguren, M.I., 2021. Cellulose nanocrystals suspensions: liquid crystal anisotropy, rheology and films iridescence. Carbohydr. Polym. 261, 117848 https://doi.org/10.1016/j.carbpol.2021.117848.

Chau, M., Sriskandha, S.E., Pichugin, D., Thérien-Aubin, H., Nykypanchuk, D., Chauve, G., Méthot, M., Bouchard, J., Gang, O., Kumacheva, E., 2015. Ion-mediated gelation of aqueous suspensions of cellulose nanocrystals. Biomacromolecules 16, 2455–2462. https://doi.org/10.1021/acs.biomac.5b00701.

Cheng, D., Wen, Y., Wang, L., An, X., Zhu, X., Ni, Y., 2015. Adsorption of polyethylene glycol (PEG) onto cellulose nano-crystals to improve its dispersity. Carbohydr. Polym. 123, 157–163. https://doi.org/10.1016/j.carbpol.2015.01.035.

Choi, K., Gao, C., Nam, J., Choi, H., 2017. Cellulose-based smart fluids under applied electric fields. Materials 10, 1060. https://doi.org/10.3390/ma10091060.

Combariza, M.Y., Martínez-Ramírez, A.P., Blanco-Tirado, C., 2021. Perspectives in nanocellulose for crude oil recovery: a minireview. Energy Fuels 35, 15381–15397. https://doi.org/10.1021/acs.energyfuels.1c02230.

Cui, S., Cui, C., Ge, S., Xie, W., Yu, M., Li, Y., Sun, Q., Xiong, L., 2022. The impact of cellulose nanocrystals on the rheology of sodium carboxymethyl cellulose and sodium alginate. J. Appl. Polym. Sci. 139 https://doi.org/10.1002/app.52919.

Dai, C., Zhao, F., 2019. Oilfield Chemistry. Springer.

De France, K.J., Yager, K.G., Hoare, T., Cranston, E.D., 2016. Cooperative ordering and kinetics of cellulose nanocrystal alignment in a magnetic field. Langmuir 32, 7564–7571. https://doi.org/10.1021/acs.langmuir.6b01827.

Derakhshandeh, B., Kerekes, R.J., Hatzikiriakos, S.G., Bennington, C.P., 2011. Rheology of pulp fibre suspensions: A critical review. Chem. Eng. Sci. 66, 3460–3470.

Dimic-Misic, K., Nieminen, K., Gane, P., Maloney, T., Sixta, H., Paltakari, J., 2014. Deriving a process viscosity for complex particulate nanofibrillar cellulose gel-containing suspensions. Appl. Rheol. 24, 43–51.

Dinand, E., Chanzy, H., Vignon, R.M., 1999. Suspensions of cellulose microfibrils from sugar beet pulp. Food Hydrocoll. 13, 275–283. https://doi.org/10.1016/S0268-005X(98)00084-8.

Dong, X.M., Gray, D.G., 1997. Effect of counterions on ordered phase formation in suspensions of charged rodlike cellulose crystallites. Langmuir 13, 2404–2409. https://doi.org/10.1021/la960724h.

Dong, Y., Xie, Y., Ma, X., Yan, L., Yu, H.-Y., Yang, M., Abdalkarim, S.Y.H., Jia, B., 2023. Multi-functional nanocellulose based nanocomposites for biodegradable food packaging: hybridization, fabrication, key properties and application. Carbohydr. Polym. 321, 121325 https://doi.org/10.1016/j.carbpol.2023.121325.

Eichhorn, S.J., 2011. Cellulose nanowhiskers: promising materials for advanced applications. Soft Matter 7, 303–315.

Facchine, E.G., Spontak, R.J., Rojas, O.J., Khan, S.A., 2020. Shear-dependent structures of flocculated micro/nanofibrillated cellulose (MNFC) in Aqueous suspensions. Biomacromolecules 21, 3561–3570. https://doi.org/10.1021/acs.biomac.0c00586.

Facchine, E.G., Bai, L., Rojas, O.J., Khan, S.A., 2021. Associative structures formed from cellulose nanofibrils and nanochitins are pH-responsive and exhibit tunable rheology. J. Colloid Interface Sci. 588, 232–241. https://doi.org/10.1016/j.jcis.2020.12.041.

Feng, S., Liu, F., Guo, Y., Ye, M., He, J., Zhou, H., Liu, L., Cai, L., Zhang, Y., Li, R., 2021. Exploring the role of chitosan in affecting the adhesive, rheological and antimicrobial properties of carboxymethyl cellulose composite hydrogels. Int. J. Biol. Macromol. 190, 554–563. https://doi.org/10.1016/j.ijbiomac.2021.08.217.

Fernandes Diniz, J.M.B., Gil, M.H., Castro, J.A.A.M., 2004. Hornification?its origin and interpretation in wood pulps. Wood Sci. Technol. 37, 489–494. https://doi.org/10.1007/s00226-003-0216-2.

Filson, P.B., Dawson-Andoh, B.E., Schwegler-Berry, D., 2009. Enzymatic-mediated production of cellulose nanocrystals from recycled pulp. Green. Chem. 11, 1808–1814.

Frka-Petesic, B., Sugiyama, J., Kimura, S., Chanzy, H., Maret, G., 2015. Negative diamagnetic anisotropy and birefringence of cellulose nanocrystals. Macromolecules 48, 8844–8857. https://doi.org/10.1021/acs.macromol.5b02201.

Fu, J., Schlenoff, J.B., 2016. Driving forces for oppositely charged polyion association in aqueous solutions: enthalpic, entropic, but not electrostatic. J. Am. Chem. Soc. 138, 980–990. https://doi.org/10.1021/jacs.5b11878.

Fukuzumi, H., Saito, T., Okita, Y., Isogai, A., 2010. Thermal stabilization of TEMPO-oxidized cellulose. Polym. Degrad. Stab. 95, 1502–1508. https://doi.org/10.1016/j.polymdegradstab.2010.06.015.

Gatenholm, P., Klemm, D., 2010. Bacterial nanocellulose as a renewable material for biomedical applications. MRS Bull. 35, 208–213. https://doi.org/10.1557/mrs2010.653.

Geng, L., Naderi, A., Mao, Y., Zhan, C., Sharma, P., Peng, X., Hsiao, B.S., 2017. Rheological properties of jute-based cellulose nanofibers under different ionic conditions. In: Agarwal, U.P., Atalla, R.H., Isogai, A. (Eds.), ACS Symposium Series. American Chemical Society, Washington, DC, pp. 113–132. https://doi.org/10.1021/bk-2017-1251.ch006.

Geng, L., Mittal, N., Zhan, C., Ansari, F., Sharma, P.R., Peng, X., Hsiao, B.S., Söderberg, L. D., 2018. Understanding the mechanistic behavior of highly charged cellulose nanofibers in aqueous systems. Macromolecules 51, 1498–1506. https://doi.org/10.1021/acs.macromol.7b02642.

Gestranius, M., Stenius, P., Kontturi, E., Sjöblom, J., Tammelin, T., 2017. Phase behaviour and droplet size of oil-in-water Pickering emulsions stabilised with plant-derived nanocellulosic materials. Colloids Surf. Physicochem. Eng. Asp. 519, 60–70.

Goodwin, J.W., Hughes, R.W., 2008. Rheology for Chemists: An Introduction. Royal Society of Chemistry.

Guo, D., Yuan, T., Sun, Q., Yan, Z., Kong, Z., Zhong, L., Zhou, Y., Sha, L., 2023. Cellulose nanofibrils as rheology modifier and fluid loss additive in water-based drilling fluids: Rheological properties, rheological modeling, and filtration mechanisms. Ind. Crop. Prod. 193, 116253.

Habibi, Y., Chanzy, H., Vignon, M.R., 2006. TEMPO-mediated surface oxidation of cellulose whiskers. Cellulose 13, 679–687.

Hackley, V.A., Ferraris, C.F., 2001. Guide to rheological nomenclature: Measurements in ceramic particulate systems. Citeseer.

Hafemann, E., Battisti, R., Bresolin, D., Marangoni, C., Machado, R.A.F., 2020. Enhancing chlorine-free purification routes of rice husk biomass waste to obtain cellulose nanocrystals. Waste Biomass Valoriz. 11, 6595–6611.

Hall, L.J., Deville, J.P., Araujo, C.S., Li, S., Rojas, O.J., 2017. Nanocellulose and its derivatives for high-performance water-based fluids, in: SPE International Conference on Oilfield Chemistry? SPE, p. D011S002R003.

He, L.I.U., Xu, J.I.N., Bin, D., 2016. Application of nanotechnology in petroleum exploration and development. Pet. Explor. Dev. 43, 1107–1115.

He, X., Lu, W., Sun, C., Khalesi, H., Mata, A., Andaleeb, R., Fang, Y., 2021. Cellulose and cellulose derivatives: Different colloidal states and food-related applications. Carbohydr. Polym. 255, 117334.

Herrick, F.W., 1984. Redispersible microfibrillated cellulose. US4481076A.

Herrick, F.W., Casebier, R.L., Hamilton, J.K., Sandberg, K.R., 1983. Microfibrillated cellulose: morphology and accessibility, in: J. Appl. Polym. Sci.: Appl. Polym. Symp.; (United States). ITT Rayonier Inc., Shelton, WA.

Hietala, M., Sain, S., Oksman, K., 2017. Highly redispersible sugar beet nanofibers as reinforcement in bionanocomposites. Cellulose 24, 2177–2189. https://doi.org/10.1007/s10570-017-1245-6.

Horozov, T.S., Binks, B.P., 2006. Particle-stabilized emulsions: a bilayer or a bridging monolayer? Angew. Chem. 118, 787–790.

Hou, J., Du, J., Sui, H., Sun, L., 2022. A review on the application of nanofluids in enhanced oil recovery. Front. Chem. Sci. Eng. 16, 1165–1197.

Hu, Z., Haruna, M., Gao, H., Nourafkan, E., Wen, D., 2017. Rheological properties of partially hydrolyzed polyacrylamide seeded by nanoparticles. Ind. Eng. Chem. Res. 56, 3456–3463. https://doi.org/10.1021/acs.iecr.6b05036.

Hubbe, M.A., 2005. Dry-strength development by polyelectrolyte complex deposition onto non-bonding glass fibres. J. Pulp Pap. Sci. 31, 159.

Hubbe, M.A., Nanko, H., McNeal, M.R., 2009. Retention aid polymer interactions with cellulosic surfaces and suspensions: a review. BioRes 4, 850–906.

Hubbe, M.A., Tayeb, P., Joyce, M., Tyagi, P., Kehoe, M., Dimic-Misic, K., Pal, L., 2017. Rheology of nanocellulose-rich aqueous suspensions: a Review. BioResources 12, 9556–9661. https://doi.org/10.15376/biores.12.4.Hubbe.

Iglesias, M.C., Shivyari, N., Norris, A., Martin-Sampedro, R., Eugenio, M.E., Lahtinen, P., Auad, M.L., Elder, T., Jiang, Z., Frazier, C.E., Peresin, M.S., 2020. The effect of residual lignin on the rheological properties of cellulose nanofibril suspensions. J. Wood Chem. Technol. 40, 370–381. https://doi.org/10.1080/02773813.2020.1828472.

Ilyin, S.O., Gorbacheva, S.N., Yadykova, A.Y., 2023. Rheology and tribology of nanocellulose-based biodegradable greases: Wear and friction protection mechanisms of cellulose microfibrils. Tribol. Int. 178, 108080.

Isaac, O.T., Pu, H., Oni, B.A., Samson, F.A., 2022. Surfactants employed in conventional and unconventional reservoirs for enhanced oil recovery—A review. Energy Rep. 8, 2806–2830.

James, A., Rahman, M.R., Mohamad Said, K.A., Kanakaraju, D., Sueraya, A.Z., Kuok, K. K., Bin Bakri, M.K., Rahman, M.M., 2023. A review of nanocellulose modification and compatibility barrier for various applications. J. Thermoplast. Compos. Mater., 08927057231205451 https://doi.org/10.1177/08927057231205451.

Jongaroontaprangsee, S., Chiewchan, N., Devahastin, S., 2018. Production of nanofibrillated cellulose with superior water redispersibility from lime residues via a chemical-free process. Carbohydr. Polym. 193, 249–258. https://doi.org/10.1016/j.carbpol.2018.04.008.

Jowkarderis, L., 2016. Carboxylated cellulose nanofibril suspensions: Rheology and mesh size analysis. McGill University (Canada).

Jowkarderis, L., van de Ven, T.G.M., 2014. Intrinsic viscosity of aqueous suspensions of cellulose nanofibrils. Cellulose 21, 2511–2517. https://doi.org/10.1007/s10570-014-0292-5.

Kaldéus, T., Nordenström, M., Carlmark, A., Wågberg, L., Malmström, E., 2018. Insights into the EDC-mediated PEGylation of cellulose nanofibrils and their colloidal stability. Carbohydr. Polym. 181, 871–878. https://doi.org/10.1016/j.carbpol.2017.11.065.

Kam, D., Braner, A., Abouzglo, A., Larush, L., Chiappone, A., Shoseyov, O., Magdassi, S., 2021. 3D printing of cellulose nanocrystal-loaded hydrogels through rapid fixation by photopolymerization. Langmuir 37, 6451–6458. https://doi.org/10.1021/acs.langmuir.1c00553.

Karakashev, S.I., Grozdanova, M.V., 2012. Foams and antifoams. Adv. Colloid Interface Sci. 176, 1–17.

Kerekes, R., Schell, C.J., 1992. Characterization of fibre flocculation regimes by a crowding factor.

Khan, N., Brettmann, B., 2018. Intermolecular interactions in polyelectrolyte and surfactant complexes in solution. Polymers 11, 51. https://doi.org/10.3390/polym11010051.

Khan, N., Zaragoza, N.Z., Travis, C.E., Goswami, M., Brettmann, B.K., 2020. Polyelectrolyte complex coacervate assembly with cellulose nanofibers. ACS Omega 5, 17129–17140. https://doi.org/10.1021/acsomega.0c00977.

Kim, J., Bang, J., Kim, Y., Kim, J.-C., Hwang, S.-W., Yeo, H., Choi, I.-G., Kwak, H.W., 2022. Eco-friendly alkaline lignin/cellulose nanofiber drying system for efficient redispersion behavior. Carbohydr. Polym. 282, 119122 https://doi.org/10.1016/j.carbpol.2022.119122.

Kim, M., Kim, S., Han, N., Lee, S., Kim, H., 2023. Understanding viscoelastic behavior of hybrid nanocellulose film based on rheological and electrostatic observation in blended suspension. Carbohydr. Polym. 300, 120218.

Kinra, S., Pal, R., 2023. Rheology of pickering emulsions stabilized and thickened by cellulose nanocrystals over broad ranges of oil and nanocrystal concentrations. Colloids Interfaces 7, 36.

Koppolu, R., Banvillet, G., Ghimire, H., Bras, J., Toivakka, M., 2022. Enzymatically pretreated high-solid-content nanocellulose for a high-throughput coating process. ACS Appl. Nano Mater. 5, 11302–11313. https://doi.org/10.1021/acsanm.2c02423.

Kropholler, H.W., Sampson, W.W., 2001. The effect of fibre length distribution on suspension crowding. J. Pulp Pap. Sci. 27, 301–305.

Kusanagi, K., Murata, S., Goi, Y., Sabi, M., Zinno, K., Kato, Y., Togashi, N., Matsuoka, T., Liang, Y., 2015. Application of cellulose nanofiber as environment-friendly polymer for oil development, in: SPE Asia Pacific Oil and Gas Conference and Exhibition. SPE, p. SPE-176456.

Laivins, G.V., Scallan, A.M., 1993. The mechanism of hornification of wood pulps. Prod. Papermak 2, 1235.

Lee, D., Oh, Y., Yoo, J.-K., Yi, J.W., Um, M.-K., Park, T., 2020. Rheological study of cellulose nanofiber disintegrated by a controlled high-intensity ultrasonication for a delicate nano-fibrillation. Cellulose 27, 9257–9269. https://doi.org/10.1007/s10570-020-03410-4.

Lee, M., Heo, M., Lee, H., Shin, J., 2021. Facile and quantitative method for estimating the isolation degree of cellulose nanocrystals (CNCs) suspensions. Materials 14, 6463.

Lee, Z.J., Tong, S., Tang, T., Lee, Y., 2022. Palm-based cellulose nanofiber isolated from mechano-chemical processing as sustainable rheological modifier in reduced fat mayonnaise. J. Food Sci. 87, 3542–3561. https://doi.org/10.1111/1750-3841.16250.

Lenfant, G., Heuzey, M.-C., van de Ven, T.G.M., Carreau, P.J., 2017. A comparative study of ECNC and CNC suspensions: effect of salt on rheological properties. Rheol. Acta 56, 51–62. https://doi.org/10.1007/s00397-016-0979-7.

Leray, N., Talantikite, M., Villares, A., Cathala, B., 2022. Xyloglucan-cellulose nanocrystal-chitosan double network hydrogels for soft actuators. Carbohydr. Polym. 293, 119753 https://doi.org/10.1016/j.carbpol.2022.119753.

Lerouge, S., Olmsted, P.D., 2020. Non-local effects in shear banding of polymeric flows. Front. Phys. 7, 246 https://doi.org/10.3389/fphy.2019.00246.

Li, M.-C., Wu, Q., Song, K., Lee, S., Qing, Y., Wu, Y., 2015a. Cellulose nanoparticles: structure–morphology–rheology relationships. ACS Sustain. Chem. Eng. 3, 821–832. https://doi.org/10.1021/acssuschemeng.5b00144.

Li, M.-C., Wu, Q., Song, K., Qing, Y., Wu, Y., 2015b. Cellulose nanoparticles as modifiers for rheology and fluid loss in bentonite water-based fluids. ACS Appl. Mater. Interfaces 7, 5006–5016. https://doi.org/10.1021/acsami.5b00498.

Li, M.-C., Tang, Z., Liu, C., Huang, R., Koo, M.S., Zhou, G., Wu, Q., 2020. Water-redispersible cellulose nanofiber and polyanionic cellulose hybrids for high-performance water-based drilling fluids. Ind. Eng. Chem. Res. 59, 14352–14363. https://doi.org/10.1021/acs.iecr.0c02644.

Li, M.-C., Wu, Q., Moon, R.J., Hubbe, M.A., Bortner, M.J., 2021. Rheological aspects of cellulose nanomaterials: governing factors and emerging applications. Adv. Mater. 33, 2006052.

Li, M.-C., Liu, X., Lv, K., Sun, J., Dai, C., Liao, B., Liu, C., Mei, C., Wu, Q., Hubbe, M., 2023a. Cellulose nanomaterials in oil and gas industry: current status and future perspectives. Prog. Mater. Sci. 139, 101187 https://doi.org/10.1016/j.pmatsci.2023.101187.

Li, Q., Wei, B., Lu, L., Li, Y., Wen, Y., Pu, W., Li, H., Wang, C., 2017. Investigation of physical properties and displacement mechanisms of surface-grafted nano-cellulose fluids for enhanced oil recovery. Fuel 207, 352–364.

Li, W., Chen, Wenxue, Wang, Z., Chen, Weijun, Zhang, M., Zhong, Q., Pei, J., Chen, H., 2022. Preparation and characterization of beads of sodium alginate/carboxymethyl chitosan/cellulose nanofiber containing porous starch embedded with gallic acid: an in vitro simulation delivery study. Foods 11, 1394. https://doi.org/10.3390/foods11101394.

Li, Z., Kang, W.-L., Li, M.-L., Yang, H.-B., Zhu, T.-Y., He, Y.-Q., Jiang, H.-Z., Zhou, B.-B., Hao, J.-T., 2023b. Surface-functionalized cellulose nanocrystals (CNC) and synergisms with surfactant for enhanced oil recovery in low-permeability reservoirs. Pet. Sci. 20, 1572–1583.

Liang, L., Yang, J., Lv, G., Lei, Z., Li, X., Liu, Q., 2021. Surface-functionalized nanocelluloses as viscosity-modifying agents in engineered cementitious composites. Front. Mater. 8, 783176.

Liu, X., Wen, Y., Qu, J., Geng, X., Chen, B., Wei, B., Wu, B., Yang, S., Zhang, H., Ni, Y., 2019. Improving salt tolerance and thermal stability of cellulose nanofibrils by grafting modification. Carbohydr. Polym. 211, 257–265.

Lowys, M.-P., Desbrières, J., Rinaudo, M., 2001. Rheological characterization of cellulosic microfibril suspensions. Role of polymeric additives. Food Hydrocoll. 15, 25–32. https://doi.org/10.1016/S0268-005X(00)00046-1.

Lu, A., Wang, Y., Boluk, Y., 2014. Investigation of the scaling law on gelation of oppositely charged nanocrystalline cellulose and polyelectrolyte. Carbohydr. Polym. 105, 214–221. https://doi.org/10.1016/j.carbpol.2014.01.077.

Lu, Y., Li, J., Ge, L., Xie, W., Wu, D., 2021. Pickering emulsion stabilized with fibrous nanocelluloses: Insight into fiber flexibility-emulsifying capacity relations. Carbohydr. Polym. 255, 117483.

Ma, G., He, M., Yang, G., Ji, X., Lucia, L.A., Chen, J., 2021. A feasible approach efficiently redisperse dried cellulose nanofibrils in water: vacuum or freeze drying in the presence of sodium chloride. Cellulose 28, 829–842. https://doi.org/10.1007/s10570-020-03591-y.

Martoïa, F., Perge, C., Dumont, P.J.J., Orgéas, L., Fardin, M.A., Manneville, S., Belgacem, M.N., 2015. Heterogeneous flow kinematics of cellulose nanofibril suspensions under shear. Soft Matter 11, 4742–4755. https://doi.org/10.1039/C5SM00530B.

Mendoza, L., Batchelor, W., Tabor, R.F., Garnier, G., 2018. Gelation mechanism of cellulose nanofibre gels: a colloids and interfacial perspective. J. Colloid Interface Sci. 509, 39–46. https://doi.org/10.1016/j.jcis.2017.08.101.

Meree, C.E., Schueneman, G.T., Meredith, J.C., Shofner, M.L., 2016. Rheological behavior of highly loaded cellulose nanocrystal/poly(vinyl alcohol) composite suspensions. Cellulose 23, 3001–3012. https://doi.org/10.1007/s10570-016-1003-1.

Mezger, T.G., 2006. The Rheology Handbook: For users of rotational and oscillatory rheometers. Vincentz Netw. GmbH Co KG Hann. Ger.

Michelin, M., Gomes, D.G., Romaní, A., Polizeli, M. de L.T.M., Teixeira, J.A., 2020. Nanocellulose production: exploring the enzymatic route and residues of pulp and paper industry. Molecules 25, 3411. https://doi.org/10.3390/molecules25153411.

Missoum, K., Bras, J., Belgacem, M.N., 2012. Water redispersible dried nanofibrillated cellulose by adding sodium chloride. Biomacromolecules 13, 4118–4125. https://doi.org/10.1021/bm301378n.

Mohtaschemi, M., Dimic-Misic, K., Puisto, A., Korhonen, M., Maloney, T., Paltakari, J., Alava, M.J., 2014. Rheological characterization of fibrillated cellulose suspensions via bucket vane viscometer. Cellulose 21, 1305–1312. https://doi.org/10.1007/s10570-014-0235-1.

Molnes, S.N., Mamonov, A., Paso, K.G., Strand, S., Syverud, K., 2018. Investigation of a new application for cellulose nanocrystals: a study of the enhanced oil recovery potential by use of a green additive. Cellulose 25, 2289–2301.

Mondal, I.H., 2015. Cellulose and Cellulose Derivatives: Synthesis, Modification and Applications. Nova Science Publishers, Incorporated.

Moon, R.J., Martini, A., Nairn, J., Simonsen, J., Youngblood, J., 2011. Cellulose nanomaterials review: structure, properties and nanocomposites. Chem. Soc. Rev. 40, 3941–3994.

de Morais Teixeira, E., Corrêa, A.C., Manzoli, A., de Lima Leite, F., de Oliveira, C.R., Mattoso, L.H.C., 2010. Cellulose nanofibers from white and naturally colored cotton fibers. Cellulose 17, 595–606.

Moser, C., Henriksson, G., Lindström, M., 2018. Improved dispersibility of once-dried cellulose nanofibers in the presence of glycerol. Nord. Pulp Pap. Res. J. 33, 647–650. https://doi.org/10.1515/npprj-2018-0054.

Naderi, A., Lindström, T., 2016. A comparative study of the rheological properties of three different nanofibrillated cellulose systems. Nord. Pulp Pap. Res. J. 31, 354–363. https://doi.org/10.3183/npprj-2016-31-p354-363.

Naderi, A., Lindström, T., Pettersson, T., 2014a. The state of carboxymethylated nanofibrils after homogenization-aided dilution from concentrated suspensions: a rheological perspective. Cellulose 21, 2357–2368. https://doi.org/10.1007/s10570-014-0329-9.

Naderi, A., Lindström, T., Sundström, J., 2014b. Carboxymethylated nanofibrillated cellulose: rheological studies. Cellulose 21, 1561–1571. https://doi.org/10.1007/s10570-014-0192-8.

Naderi, A., Lindström, T., Sundström, J., Flodberg, G., 2015a. Can redispersible low-charged nanofibrillated cellulose be produced by the addition of carboxymethyl cellulose? Nord. Pulp Pap. Res. J. 30, 568–577. https://doi.org/10.3183/npprj-2015-30-04-p568-577.

Naderi, A., Lindström, T., Sundström, J., Pettersson, T., Flodberg, G., Erlandsson, J., 2015b. Microfluidized carboxymethyl cellulose modified pulp: a nanofibrillated cellulose system with some attractive properties. Cellulose 22, 1159–1173.

Nang An, V., Nhan, C., Thuc, H., Tap, T.D., Van, T.T.T., Van Viet, P., Van Hieu, L., 2020. Extraction of high crystalline nanocellulose from biorenewable sources of Vietnamese agricultural wastes. J. Polym. Environ. 28, 1465–1474.

Nazari, B., Kumar, V., Bousfield, D.W., Toivakka, M., 2016. Rheology of cellulose nanofibers suspensions: Boundary driven flow. J. Rheol. 60, 1151–1159. https://doi.org/10.1122/1.4960336.

Nechyporchuk, O., Belgacem, M.N., Pignon, F., 2014. Rheological properties of micro-/nanofibrillated cellulose suspensions: Wall-slip and shear banding phenomena. Carbohydr. Polym. 112, 432–439. https://doi.org/10.1016/j.carbpol.2014.05.092.

Nechyporchuk, O., Belgacem, M.N., Pignon, F., 2015. Concentration effect of TEMPO-oxidized nanofibrillated cellulose aqueous suspensions on the flow instabilities and small-angle X-ray scattering structural characterization. Cellulose 22, 2197–2210. https://doi.org/10.1007/s10570-015-0640-0.

Nechyporchuk, O., Belgacem, M.N., Bras, J., 2016a. Production of cellulose nanofibrils: a review of recent advances. Ind. Crops Prod. 93, 2–25. https://doi.org/10.1016/j.indcrop.2016.02.016.

Nechyporchuk, O., Belgacem, M.N., Pignon, F., 2016b. Current progress in rheology of cellulose nanofibril suspensions. Biomacromolecules 17, 2311–2320. https://doi.org/10.1021/acs.biomac.6b00668.

Neibolts, N., Platnieks, O., Gaidukovs, S., Barkane, A., Thakur, V.K., Filipova, I., Mihai, G., Zelca, Z., Yamaguchi, K., Enachescu, M., 2020. Needle-free electrospinning of nanofibrillated cellulose and graphene nanoplatelets based sustainable poly (butylene succinate) nanofibers. Mater. Today Chem. 17, 100301 https://doi.org/10.1016/j.mtchem.2020.100301.

Nordenström, M., Kaldéus, T., Erlandsson, J., Pettersson, T., Malmström, E., Wågberg, L., 2021. Redispersion strategies for dried cellulose nanofibrils. ACS Sustain. Chem. Eng. 9, 11003–11010. https://doi.org/10.1021/acssuschemeng.1c02122.

Nyamayaro, K., Mehrkhodavandi, P., Hatzikiriakos, S.G., 2023. Impact of counterion valency on the rheology of sulfonated cellulose nanocrystal hydrogels. Carbohydr. Polym. 302, 120378 https://doi.org/10.1016/j.carbpol.2022.120378.

Oguzlu, H., Danumah, C., Boluk, Y., 2016. The role of dilute and semi-dilute cellulose nanocrystal (CNC) suspensions on the rheology of carboxymethyl cellulose (CMC) solutions. Can. J. Chem. Eng. 94, 1841–1847. https://doi.org/10.1002/cjce.22597.

Oguzlu, H., Danumah, C., Boluk, Y., 2017. Colloidal behavior of aqueous cellulose nanocrystal suspensions. Curr. Opin. Colloid Interface Sci. 29, 46–56. https://doi.org/10.1016/j.cocis.2017.02.002.

Olmos-Juste, R., Alonso-Lerma, B., Pérez-Jiménez, R., Gabilondo, N., Eceiza, A., 2021. 3D printed alginate-cellulose nanofibers based patches for local curcumin administration. Carbohydr. Polym. 264, 118026 https://doi.org/10.1016/j.carbpol.2021.118026.

Ovarlez, G., Rodts, S., Chateau, X., Coussot, P., 2009. Phenomenology and physical origin of shear localization and shear banding in complex fluids. Rheol. Acta 48, 831–844. https://doi.org/10.1007/s00397-008-0344-6.

Pääkkö, M., Ankerfors, M., Kosonen, H., Nykänen, A., Ahola, S., Österberg, M., Ruokolainen, J., Laine, J., Larsson, P.T., Ikkala, O., Lindström, T., 2007. Enzymatic hydrolysis combined with mechanical shearing and high-pressure homogenization for nanoscale cellulose fibrils and strong gels. Biomacromolecules 8, 1934–1941. https://doi.org/10.1021/bm061215p.

Parajuli, S., Alazzam, O., Wang, M., Mota, L.C., Adhikari, S., Wicks, D., Ureña-Benavides, E.E., 2020. Surface properties of cellulose nanocrystal stabilized crude oil emulsions and their effect on petroleum biodegradation. Colloids Surf. Physicochem. Eng. Asp. 596, 124705.

Parker, R.M., Guidetti, G., Williams, C.A., Zhao, T., Narkevicius, A., Vignolini, S., Frka-Petesic, B., 2018. The self-assembly of cellulose nanocrystals: Hierarchical design of visual appearance. Adv. Mater. 30, 1704477.

Peng, Y., Via, B., 2021. The effect of cellulose nanocrystal suspension treatment on suspension viscosity and casted film property. Polymers 13, 2168. https://doi.org/10.3390/polym13132168.

Petzold, G., Schwarz, S., 2013. Polyelectrolyte complexes in flocculation applications. In: Müller, M. (Ed.), Polyelectrolyte Complexes in the Dispersed and Solid State II, Advances in Polymer Science. Springer Berlin Heidelberg, Berlin, Heidelberg, pp. 25–65. https://doi.org/10.1007/12_2012_205.

Platnieks, O., Sereda, A., Gaidukovs, S., Thakur, V.K., Barkane, A., Gaidukova, G., Filipova, I., Ogurcovs, A., Fridrihsone, V., 2021. Adding value to poly (butylene succinate) and nanofibrillated cellulose-based sustainable nanocomposites by applying masterbatch process. Ind. Crops Prod. 169, 113669 https://doi.org/10.1016/j.indcrop.2021.113669.

, 2014Polyelectrolyte Complexes in the Dispersed and Solid State II M. Müller Advances in Polymer Science 2014 Springer Berlin Heidelberg Berlin, Heidelberg doi: 10.1007/978-3-642-40746-8.

Prathapan, R., Thapa, R., Garnier, G., Tabor, R.F., 2016. Modulating the zeta potential of cellulose nanocrystals using salts and surfactants. Colloids Surf. Physicochem. Eng. Asp. 509, 11–18.

Qi, W., Yu, J., Zhang, Z., Xu, H.-N., 2019. Effect of pH on the aggregation behavior of cellulose nanocrystals in aqueous medium. Mater. Res. Express 6, 125078. https://doi.org/10.1088/2053-1591/ab5974.

Qi, Y., Wang, S., Liza, A.A., Li, J., Yang, G., Zhu, W., Song, J., Xiao, H., Li, H., Guo, J., 2023. Controlling the nanocellulose morphology by preparation conditions. Carbohydr. Polym., 121146

Qing, Y., Sabo, R., Zhu, J.Y., Agarwal, U., Cai, Z., Wu, Y., 2013. A comparative study of cellulose nanofibrils disintegrated via multiple processing approaches. Carbohydr. Polym. 97, 226–234.

Raj, P., Varanasi, S., Batchelor, W., Garnier, G., 2015. Effect of cationic polyacrylamide on the processing and properties of nanocellulose films. J. Colloid Interface Sci. 447, 113–119. https://doi.org/10.1016/j.jcis.2015.01.019.

Rana, A.K., 2022. Green approaches in the valorization of plant wastes: recent insights and future directions. Curr. Opin. Green. Sustain. Chem., 100696

Rana, A.K., 2023. Nanocellulose-based hydrogels: preparation strategies, dye adsorption and factors impacting. Nanofabrication 8. https://doi.org/10.37819/nanofab.8.1757.

Rana, A.K., Thakur, V.K., 2021. The bright side of cellulosic Hibiscus sabdariffa fibres: towards sustainable materials from the macro-to nano-scale. Mater. Adv. 2, 4945–4965.

Rana, A.K., Thakur, V.K., 2023. Impact of physico-chemical properties of nanocellulose on rheology of aqueous suspensions and its utility in multiple fields: A review. J. Vinyl Addit. Technol. 29, 617–648. https://doi.org/10.1002/vnl.22006.

Rana, A.K., Guleria, S., Gupta, V.K., Thakur, V.K., 2022a. Cellulosic pine needles-based biorefinery for a circular bioeconomy. Bioresour. Technol., 128255

Rana, A.K., Gupta, V.K., Newbold, J., Roberts, D., Rees, R.M., Krishnamurthy, S., Thakur, V.K., 2022b. Sugar beet pulp: Resurgence and trailblazing journey towards a circular bioeconomy. Fuel 312, 122953.

Rana, A.K., Scarpa, F., Thakur, V.K., 2022c. Cellulose/polyaniline hybrid nanocomposites: Design, fabrication, and emerging multidimensional applications. Ind. Crop. Prod. 187, 115356.

Rana, A.K., Gupta, V.K., Hart, P., Thakur, V.K., 2024. Cellulose-alginate hydrogels and their nanocomposites for water remediation and biomedical applications. Environ. Res. 243, 117889 https://doi.org/10.1016/j.envres.2023.117889.

Rana, A.K., Gupta, V.K., Saini, A.K., Voicu, S.I., Abdellattifaand, M.H., Thakur, V.K., 2021a. Water desalination using nanocelluloses/cellulose derivatives based membranes for sustainable future. Desalination 520, 115359. https://doi.org/10.1016/j.desal.2021.115359.

Rana, A.K., Mishra, Y.K., Gupta, V.K., Thakur, V.K., 2021b. Sustainable materials in the removal of pesticides from contaminated water: Perspective on macro to nanoscale cellulose. Sci. Total Environ. 797, 149129 https://doi.org/10.1016/j.scitotenv.2021.149129.

Rana, A.K., Potluri, P., Thakur, V.K., 2021c. Cellulosic grewia optiva fibres: towards chemistry, surface engineering and sustainable materials. J. Environ. Chem. Eng. 9, 106059 https://doi.org/10.1016/j.jece.2021.106059.

Rana, A.K., Frollini, E., Thakur, V.K., 2021. Cellulose nanocrystals: pretreatments, preparation strategies, and surface functionalization. Int. J. Biol. Macromol. 182, 1554–1581. https://doi.org/10.1016/j.ijbiomac.2021.05.119.

Raza, S., Gates, I.D., 2021. Effect of cellulose nanocrystal nanofluid on displacement of oil in a Hele-Shaw cell. J. Pet. Sci. Eng. 196, 108068.

Reid, M.S., Marway, H.S., Moran-Hidalgo, C., Villalobos, M., Cranston, E.D., 2017. Comparison of polyethylene glycol adsorption to nanocellulose versus fumed silica in water. Cellulose 24, 4743–4757. https://doi.org/10.1007/s10570-017-1482-8.

Ren, Q., Wu, M., Wang, L., Zheng, W., Hikima, Y., Semba, T., Ohshima, M., 2022. Cellulose nanofiber reinforced poly (lactic acid) with enhanced rheology, crystallization and foaming ability. Carbohydr. Polym. 286, 119320 https://doi.org/10.1016/j.carbpol.2022.119320.

Revol, J.-F., Marchessault, R.H., 1993. In vitro chiral nematic ordering of chitin crystallites. Int. J. Biol. Macromol. 15, 329–335. https://doi.org/10.1016/0141-8130(93)90049-R.

Revol, J.-F., Bradford, H., Giasson, J., Marchessault, R.H., Gray, D.G., 1992. Helicoidal self-ordering of cellulose microfibrils in aqueous suspension. Int. J. Biol. Macromol. 14, 170–172.

Rezayati Charani, P., Dehghani-Firouzabadi, M., Afra, E., Shakeri, A., 2013. Rheological characterization of high concentrated MFC gel from kenaf unbleached pulp. Cellulose 20, 727–740. https://doi.org/10.1007/s10570-013-9862-1.

Rissanen, V., Vajravel, S., Kosourov, S., Arola, S., Kontturi, E., Allahverdiyeva, Y., Tammelin, T., 2021. Nanocellulose-based mechanically stable immobilization matrix for enhanced ethylene production: a framework for photosynthetic solid-state cell factories. Green. Chem. 23, 3715–3724. https://doi.org/10.1039/D1GC00502B.

Roberts, J.C., 2007. The Chemistry of Paper. Royal Society of Chemistry.

Saarikoski, E., Saarinen, T., Salmela, J., Seppälä, J., 2012. Flocculated flow of microfibrillated cellulose water suspensions: an imaging approach for characterisation of rheological behaviour. Cellulose 19, 647–659. https://doi.org/10.1007/s10570-012-9661-0.

Saarinen, T., Lille, M., Seppälä, J., 2009. Technical aspects on rheological characterization of microfibrillar cellulose water suspensions 98. T. Saarinen, M. Lille, J. Seppälä. Annu Trans – Nord Rheol Soc 17, 121.

Saito, T., Kimura, S., Nishiyama, Y., Isogai, A., 2007. Cellulose nanofibers prepared by TEMPO-mediated oxidation of native cellulose. Biomacromolecules 8, 2485–2491. https://doi.org/10.1021/bm0703970.

Sandell, L.S., Luner, P., 1974. Flocculation of microcrystalline cellulose with cationic ionene polymers. J. Appl. Polym. Sci. 18, 2075–2083. https://doi.org/10.1002/app.1974.070180716.

Sang, X., Qin, C., Tong, Z., Kong, S., Jia, Z., Wan, G., Liu, X., 2017. Mechanism and kinetics studies of carboxyl group formation on the surface of cellulose fiber in a TEMPO-mediated system. Cellulose 24, 2415–2425.

Satyamurthy, P., Jain, P., Balasubramanya, R.H., Vigneshwaran, N., 2011. Preparation and characterization of cellulose nanowhiskers from cotton fibres by controlled microbial hydrolysis. Carbohydr. Polym. 83, 122–129.

Schenker, M., Schoelkopf, J., Gane, P., Mangin, P., 2018. Influence of shear rheometer measurement systems on the rheological properties of microfibrillated cellulose (MFC) suspensions. Cellulose 25, 961–976. https://doi.org/10.1007/s10570-017-1642-x.

Shafiei-Sabet, S., Hamad, W.Y., Hatzikiriakos, S.G., 2012. Rheology of Nanocrystalline Cellulose Aqueous Suspensions. Langmuir 28, 17124–17133. https://doi.org/10.1021/la303380v.

Shafiei-Sabet, S., Hamad, W.Y., Hatzikiriakos, S.G., 2014. Ionic strength effects on the microstructure and shear rheology of cellulose nanocrystal suspensions. Cellulose 21, 3347–3359. https://doi.org/10.1007/s10570-014-0407-z.

Shafiei-Sabet, S., Martinez, M., Olson, J., 2016. Shear rheology of micro-fibrillar cellulose aqueous suspensions. Cellulose 23, 2943–2953. https://doi.org/10.1007/s10570-016-1040-9.

Shin, S., Hyun, J., 2021. Rheological properties of cellulose nanofiber hydrogel for high-fidelity 3D printing. Carbohydr. Polym. 263, 117976 https://doi.org/10.1016/j.carbpol.2021.117976.

Sim, K., Lee, J., Lee, H., Youn, H.J., 2015. Flocculation behavior of cellulose nanofibrils under different salt conditions and its impact on network strength and dewatering ability. Cellulose 22, 3689–3700. https://doi.org/10.1007/s10570-015-0784-y.

Singha, A.S., Thakur, V.K., 2009. Synthesis, characterisation and analysis of hibiscus sabdariffa fibre reinforced polymer matrix based composites. Polym. Polym. Compos. 17, 189–194. https://doi.org/10.1177/096739110901700308.

Sugiyama, J., Chanzy, H., Maret, G., 1992. Orientation of cellulose microcrystals by strong magnetic fields. Macromolecules 25, 4232–4234. https://doi.org/10.1021/ma00042a032.

T, L., 1982. The effect of carboxyl groups and their ionic form during drying on the hornification of cellulose fibers. Sven. Pap. 85, R146–R151.

Tanaka, R., Saito, T., Ishii, D., Isogai, A., 2014. Determination of nanocellulose fibril length by shear viscosity measurement. Cellulose 21, 1581–1589. https://doi.org/10.1007/s10570-014-0196-4.

Tang, J.X., Wong, S., Tran, P.T., Janmey, P.A., 1996. Counterion induced bundle formation of rodlike polyelectrolytes. Ber. Bunsenges. Für Phys. Chem. 100, 796–806. https://doi.org/10.1002/bbpc.19961000620.

Tang, Y., Wang, X., Huang, B., Wang, Z., Zhang, N., 2018. Effect of Cationic Surface Modification on the Rheological Behavior and Microstructure of Nanocrystalline Cellulose. Polymers 10, 278. https://doi.org/10.3390/polym10030278.

Tardy, B.L., Yokota, S., Ago, M., Xiang, W., Kondo, T., Bordes, R., Rojas, O.J., 2017. Nanocellulose–surfactant interactions. Curr. Opin. Colloid Interface Sci. 29, 57–67. https://doi.org/10.1016/j.cocis.2017.02.004.

Thakur, V.K., Singha, A.S., Thakur, M.K., 2013. Fabrication and Physico-Chemical Properties of High-Performance Pine Needles/Green Polymer Composites. Int. J. Polym. Mater. Polym. Biomater. 62, 226–230. https://doi.org/10.1080/00914037.2011.641694.

Tingaut, P., Zimmermann, T., Sèbe, G., 2012. Cellulose nanocrystals and microfibrillated cellulose as building blocks for the design of hierarchical functional materials. J. Mater. Chem. 22, 20105–20111.

Trache, D., Tarchoun, A.F., Derradji, M., Hamidon, T.S., Masruchin, N., Brosse, N., Hussin, M.H., 2020. Nanocellulose: from fundamentals to advanced applications. Front. Chem. 8, 392.

ÜNAL KIZILIRMAK, C., 2023. NANOCELLULOSE AS AN ENHANCED OIL RECOVERY AGENT FOR CARBONATE RESERVOIRS.

Vadodaria, S.S., Onyianta, A.J., Sun, D., 2018. High-shear rate rheometry of micro-nanofibrillated cellulose (CMF/CNF) suspensions using rotational rheometer. Cellulose 25, 5535–5552. https://doi.org/10.1007/s10570-018-1963-4.

Vanderfleet, O.M., Osorio, D.A., Cranston, E.D., 2018. Optimization of cellulose nanocrystal length and surface charge density through phosphoric acid hydrolysis. Philos. Trans. R. Soc. Math. Phys. Eng. Sci. 376, 20170041.

Vickers, Z., Damodhar, H., Grummer, C., Mendenhall, H., Banaszynski, K., Hartel, R., Hind, J., Joyce, A., Kaufman, A., Robbins, J., 2015. Relationships Among Rheological, Sensory Texture, and Swallowing Pressure Measurements of Hydrocolloid-Thickened Fluids. Dysphagia 30, 702–713. https://doi.org/10.1007/s00455-015-9647-9.

Wahlkrantz, E., 2020. Method development for rheological characterization of microfibrillated cellulose.

Wang, K., Sui, J., Gao, W., Yu, B., Yuan, C., Guo, L., Cui, B., Abd El-Aty, A.M., 2022a. Effects of xanthan gum and sodium alginate on gelatinization and gels structure of debranched pea starch by pullulanase. Food Hydrocoll. 130, 107733 https://doi.org/10.1016/j.foodhyd.2022.107733.

Wang, R., Rosen, T., Zhan, C., Chodankar, S., Chen, J., Sharma, P.R., Sharma, S.K., Liu, T., Hsiao, B.S., 2019. Morphology and Flow Behavior of Cellulose Nanofibers Dispersed in Glycols. Macromolecules 52, 5499–5509. https://doi.org/10.1021/acs.macromol.9b01036.

Wang, S., Li, K., Xia, T., Lan, P., Xu, H., Lin, N., 2022b. Chemical grafting fluoropolymer on cellulose nanocrystals and its rheological modification to perfluoropolyether oil. Carbohydr. Polym. 276, 118802 https://doi.org/10.1016/j.carbpol.2021.118802.

Wang, X., Lei, Q., Luo, J., Wang, P., Xiao, P., Ye, Y., Wu, X., Liu, Y., Zhang, G., 2021. Application of nanocellulose in oilfield chemistry. ACS Omega 6, 20833–20845.

Wani, O.B., Shoaib, M., Al Sumaiti, A., Bobicki, E.R., Alhassan, S.M., 2020. Application of Green additives for enhanced oil recovery: cellulosic nanocrystals as fluid diversion agents in carbonate reservoirs. Colloids Surf. Physicochem. Eng. Asp. 589, 124422.

Warwar Damouny, C., Martin, P., Vasilyev, G., Vilensky, R., Fadul, R., Redenski, I., Srouji, S., Zussman, E., 2022. Injectable Hydrogels Based on Inter-Polyelectrolyte Interactions between Hyaluronic Acid, Gelatin, and Cationic Cellulose Nanocrystals. Biomacromolecules 23, 3222–3234. https://doi.org/10.1021/acs.biomac.2c00316.

Wei, B., Li, H., Li, Q., Lu, L., Li, Y., Pu, W., Wen, Y., 2018. Investigation of synergism between surface-grafted nano-cellulose and surfactants in stabilized foam injection process. Fuel 211, 223–232.

Wei, B., Wang, Y., Mao, R., Xu, X., Wood, C., Wen, Y., 2019. Design of nanocellulose fibrils containing lignin segment (L-NCF) for producing stable liquid foams as "green" flooding agents for oil recovery. ACS Sustain. Chem. Eng. 7, 11426–11437.

Wijaya, C.J., Ismadji, S., Aparamarta, H.W., Gunawan, S., 2020. Hydrophobic modification of cellulose nanocrystals from bamboo shoots using rarasaponins. ACS Omega 5, 20967–20975.

Wu, C., McClements, D.J., Li, L., He, M., Li, Y., Teng, F., 2022. Fabrication of composite hydrogels by assembly of okara cellulose nanofibers and gum Arabic in ionic liquids: structure and properties. J. Mol. Liq. 349, 118132 https://doi.org/10.1016/j.molliq.2021.118132.

Xhanari, K., Syverud, K., Chinga-Carrasco, G., Paso, K., Stenius, P., 2011. Structure of nanofibrillated cellulose layers at the o/w interface. J. Colloid Interface Sci. 356, 58–62.

Xu, J., Wang, P., Yuan, B., Zhang, H., 2024. Rheology of cellulose nanocrystal and nanofibril suspensions. Carbohydr. Polym. 324, 121527 https://doi.org/10.1016/j.carbpol.2023.121527.

Xu, L., Liu, S., Qiu, Z., Gong, H., Fan, H., Zhu, T., Zhang, H., Dong, M., 2021. Hydrophobic effect further improves the rheological behaviors and oil recovery of polyacrylamide/nanosilica hybrids at high salinity. Chem. Eng. Sci. 232, 116369 https://doi.org/10.1016/j.ces.2020.116369.

Xu, Y., Salmi, J., Kloser, E., Perrin, F., Grosse, S., Denault, J., Lau, P.C., 2013. Feasibility of nanocrystalline cellulose production by endoglucanase treatment of natural bast fibers. Ind. Crops Prod. 51, 381–384.

Xu, Y., Atrens, A.D., Stokes, J.R., 2017. Rheology and microstructure of aqueous suspensions of nanocrystalline cellulose rods. J. Colloid Interface Sci. 496, 130–140. https://doi.org/10.1016/j.jcis.2017.02.020.

Xu, Y., Atrens, A.D., Stokes, J.R., 2019. Liquid crystal hydroglass formed via phase separation of nanocellulose colloidal rods. Soft Matter 15, 1716–1720.

Yamagata, Y., Niinobe, S., Suga, K., Nakano, Y., Miyamoto, K., 2022. Rheological and rheo-optical behaviors of nanocellulose suspensions containing unfibrillated fibers. Cellulose 29, 3703–3719.

Yuan, J., Liu, D., Huang, W., Li, J., Tang, H., Jia, Haidong, Wang, J., Song, L., Huang, P., Jia, Han, 2021. Effects of Various Nanoparticles on the Rheological Properties of Carboxylic Cellulose Nanofibers and the Compound System's Application in Enhanced Oil Recovery. Energy Fuels 35, 11295–11305. https://doi.org/10.1021/acs.energyfuels.1c01377.

Zhang, Y., Yang, S., Tang, H., Wan, S., Qin, W., Zeng, Q., Huang, J., Yu, G., Feng, Y., Li, J., 2022. Depletion stabilization of emulsions based on bacterial cellulose/carboxymethyl chitosan complexes. Carbohydr. Polym. 297, 119904 https://doi.org/10.1016/j.carbpol.2022.119904.

Zhou, S., Song, J., Xu, M., Xu, P., You, F., Pu, L., 2023. Rheological and filtration properties of water-based drilling fluids as influenced by cellulose nanomaterials: different aspect ratios and modified groups. Cellulose 30, 3667–3683.

Zhu, H., De Kee, D., 2008. Double concentric cylinder geometry with slotted rotor to measure the yield stress of complex systems: a numerical study. J. Rheol. 52, 913–922.

Zhu, J., Xie, S., Yang, Z., Li, X., Chen, J., Zhang, X., Zheng, N., 2021. A review of recent advances and prospects on nanocellulose properties and its applications in oil and gas production. J. Nat. Gas. Sci. Eng. 96, 104253.

Zhu, Q., Yao, Q., Sun, J., Chen, H., Xu, W., Liu, J., Wang, Q., 2020. Stimuli induced cellulose nanomaterials alignment and its emerging applications: a review. Carbohydr. Polym. 230, 115609 https://doi.org/10.1016/j.carbpol.2019.115609.

Zielińska, D., Rydzkowski, T., Thakur, V.K., Borysiak, S., 2021. Enzymatic engineering of nanometric cellulose for sustainable polypropylene nanocomposites. Ind. Crop. Prod. 161, 113188 https://doi.org/10.1016/j.indcrop.2020.113188.